




Review

Crystal Chemistry and Structural Complexity of Natural and Synthetic Uranyl Selenites

Vladislav V. Gurzhiy ^{1,*}, Ivan V. Kuporev ¹, Vadim M. Kovrugin ¹, Mikhail N. Murashko ¹, Anatoly V. Kasatkin ² and Jakub Plášil ³

¹ Institute of Earth Sciences, St. Petersburg State University, University Emb. 7/9, St. Petersburg 199034, Russian; st054910@student.spbu.ru (I.V.K.); kovrugin_vm@hotmail.com (V.M.K.); mzmurashko@gmail.com (M.N.M.)

² Fersman Mineralogical Museum of the Russian Academy of Sciences, Leninskiy pr. 18, 2, Moscow 119071, Russian; kasatkin@inbox.ru

³ Institute of Physics, The Academy of Sciences of the Czech Republic, v.v.i., Na Slovance 2, 18221 Praha 8, Czech Republic; plasil@fzu.cz

* Correspondence: vladislav.gurzhiy@spbu.ru or vladgeo17@mail.ru

Received: 10 November 2019; Accepted: 28 November 2019; Published: 30 November 2019



Abstract: Comparison of the natural and synthetic phases allows an overview to be made and even an understanding of the crystal growth processes and mechanisms of the particular crystal structure formation. Thus, in this work, we review the crystal chemistry of the family of uranyl selenite compounds, paying special attention to the pathways of synthesis and topological analysis of the known crystal structures. Comparison of the isotypic natural and synthetic uranyl-bearing compounds suggests that uranyl selenite mineral formation requires heating, which most likely can be attributed to the radioactive decay. Structural complexity studies revealed that the majority of synthetic compounds have the topological symmetry of uranyl selenite building blocks equal to the structural symmetry, which means that the highest symmetry of uranyl complexes is preserved regardless of the interstitial filling of the structures. Whereas the real symmetry of U-Se complexes in the structures of minerals is lower than their topological symmetry, which means that interstitial cations and H₂O molecules significantly affect the structural architecture of natural compounds. At the same time, structural complexity parameters for the whole structure are usually higher for the minerals than those for the synthetic compounds of a similar or close organization, which probably indicates the preferred existence of such natural-born architectures. In addition, the reexamination of the crystal structures of two uranyl selenite minerals guilleminite and demesmaeckerite is reported. As a result of the single crystal X-ray diffraction analysis of demesmaeckerite, Pb₂Cu₅[(UO₂)₂(SeO₃)₆(OH)₆](H₂O)₂, the H atoms positions belonging to the interstitial H₂O molecules were assigned. The refinement of the guilleminite crystal structure allowed the determination of an additional site arranged within the void of the interlayer space and occupied by an H₂O molecule, which suggests the formula of guilleminite to be written as Ba[(UO₂)₃(SeO₃)₂O₂](H₂O)₄ instead of Ba[(UO₂)₃(SeO₃)₂O₂](H₂O)₃.

Keywords: uranyl; selenite; selenate; crystal structure; topology; structural complexity; demesmaeckerite; guilleminite; haynesite

1. Introduction

All natural compounds of U(VI) and selenium are selenites. Uranyl selenites can be justifiably attributed to rare mineral species. Nowadays, there are only seven uranyl selenite mineral species approved by the International Mineralogical Association as of 20 October 2019 (for comparison, there are >40 uranyl sulfates and ~50 uranyl phosphates): Guilleminite, Ba[(UO₂)₃(SeO₃)₂O₂](H₂O)₃ [1],

demesmaeckerite, $\text{Pb}_2\text{Cu}_5[(\text{UO}_2)_2(\text{SeO}_3)_6(\text{OH})_6](\text{H}_2\text{O})_2$ [2], marthozite, $\text{Cu}[(\text{UO}_2)_3(\text{SeO}_3)_2\text{O}_2](\text{H}_2\text{O})_8$ [3], derriksite, $\text{Cu}_4[(\text{UO}_2)(\text{SeO}_3)_2](\text{OH})_6$ [4], haynesite, $[(\text{UO}_2)_3(\text{SeO}_3)_2(\text{OH})_2](\text{H}_2\text{O})_5$ [5], piretite, $\text{Ca}(\text{UO}_2)_3(\text{SeO}_3)_2(\text{OH})_4 \cdot 4\text{H}_2\text{O}$ [6], and larisaitite, $\text{Na}(\text{H}_3\text{O})[(\text{UO}_2)_3(\text{SeO}_3)_2\text{O}_2](\text{H}_2\text{O})_4$ [7]. Their occurrence is limited to just a few localities. First, these are Musonoi and Shinkolobwe mines in DR Congo [6], two of the minerals were only found in the Repete mine (San Juan County, Utah, USA) [5], and a few more occurrences in Europe could be mentioned (small uranium deposit Zálesí in the Czech Republic, Liauzun in France, and La Creusaz U prospect in Switzerland) [8]. Nevertheless, apart from mineralogy, uranyl selenites are of great interest from the geochemical and radiochemical points of view. It is known that fission products contain 53 g per ton [9] of long-lived ^{79}Se isotope with a half-life of 1.1×10^6 years [10] after three years of nuclear fuel irradiation in the reactor. Thus, an understanding of the processes of mineral formation in nature and their synthetic analogs in laboratories can help in the processing of nuclear wastes. Crystal chemical and structural investigations are key points in such a material's scientific studies due to the essential knowledge of how the variation in the chemical composition and growth conditions affects the crystal structure formation.

Herein, we review the topological diversity and growth conditions of natural and synthetic uranyl selenites. Crystal structures of two uranyl selenite minerals guilleminite and demesmaeckerite were refined. The structural complexity approach was implemented to determine the preference of a particular topological type, taking into account existing geometrical isomers.

2. Materials and Methods

2.1. Occurrence

The samples of minerals studied in this work were taken from the Fersman Mineralogical Museum, Museum of Natural History in Luxembourg and private collections of authors of the current paper (V.V.G., A.V.K.). Guilleminite: from the Museum (69465 and 82312), from V.V.G. (6111). Demesmaeckerite: from J.P. Haynesite: from the Fersman Museum (88922 and 94267), from V.V.G. (5767), from A.V.K. (247X). The samples of guilleminite and demesmaeckerite originate from the Musonoi, DR Congo. The samples of haynesite originate from the Repete mine, Utah, UT, USA.

2.2. Single-Crystal X-Ray Diffraction Study

A single crystal of guilleminite ($0.08 \times 0.04 \times 0.01 \text{ mm}^3$) was selected under binoculars, encased in viscous cryoprotectant, and mounted on cryo-loop. Diffraction data were collected using a Bruker Kappa Duo diffractometer (Bruker AXS, Madison, WI, USA) equipped with a CCD (charge-coupled device) Apex II detector operated with monochromated microfocused $\text{MoK}\alpha$ radiation ($\lambda[\text{MoK}\alpha] = 0.71073 \text{ \AA}$) at 45 kV and 0.6 mA. Diffraction data were collected at 100 K with frame widths of 0.5° in ω and φ , and an exposure of 70 s per frame. Diffraction data were integrated, and background, Lorentz, and polarization correction were applied. An empirical absorption correction based on spherical harmonics implemented in the SCALE3 ABSPACK algorithm was applied in the CrysAlisPro program [11]. The unit-cell parameters were refined using the least-squares techniques. The crystal structure of guilleminite was solved by a dual-space algorithm and refined using the SHELX programs [12,13] incorporated in the OLEX2 program package [14]. The final model includes coordinates and anisotropic displacement parameters for all non-H atoms. The H atoms of H_2O molecules were localized from difference Fourier maps and were included in the refinement, with $U_{\text{iso}}(\text{H})$ set to $1.5U_{\text{eq}}(\text{O})$ and O–H restrained to 0.95 \AA .

A dark-olive green prismatic crystal of demesmaeckerite ($0.034 \times 0.032 \times 0.022 \text{ mm}^3$) was mounted on a glass fiber, and diffraction intensities were measured at room temperature with a Rigaku SuperNova (Oxford, UK) single-crystal diffractometer. The diffraction experiment was done using $\text{MoK}\alpha$ radiation from a micro-focus X-ray source collimated and monochromatized by mirror-optics and the detection of the reflected X-rays was done by an Atlas S2 CCD detector. X-ray diffraction data were collected at room-temperature with frame widths of 1.0° in ω and an exposure of 80 s per

frame. Diffraction data were integrated, and background, Lorentz, and polarization correction were applied. An empirical absorption correction based on spherical harmonics implemented in the SCALE3 ABSPACK algorithm was applied in the CrysAlisPro program [11]. The structure was solved by the charge-flipping algorithm [12] and refined using the Jana2006 program [15]. The final refinement cycles were undertaken considering all atoms (except of hydrogen) refined with anisotropic atomic displacement parameters. The H atoms of H₂O molecules were localized from the difference Fourier maps and were subsequently refined with $U_{\text{iso}}(\text{H})$ set to $1.2 \cdot U_{\text{eq}}$ of the donor O atom and O–H softly restrained to 0.95 Å.

Supplementary crystallographic data were deposited in the Inorganic Crystal Structure Database (ICSD) and can be obtained by quoting the depository numbers CSD 1963864 and 1964420 for guilleminite and demesmaekerite, respectively, at <https://www.ccdc.cam.ac.uk/structures/> (see Supplementary Materials).

2.3. Coordination of U and Se

The crystal structures of all the natural and synthetic compounds described herein are based on the chained or layered substructural units built by the linkage of U- and Se-centered coordination polyhedra. U(VI) atoms form approximately linear UO_2^{2+} uranyl ions (*Ur*) with two short $\text{U}^{6+} \equiv \text{O}^{2-}$ bonds. *Ur* cation is coordinated in the equatorial plane by other four to six oxygen atoms, to form a tetra-, penta-, or hexagonal bipyramid, respectively, as a coordination polyhedron of U^{6+} atoms. The selenite group has a configuration of a trigonal pyramid with its apical vertex occupied by the Se^{4+} cation possessing a stereochemically active lone-electron pair. In the crystal structures of number of synthetic uranyl selenium compounds, there are also Se(VI) species that form $[\text{SeO}_4]^{2-}$ tetrahedra.

2.4. Graphical Representation and Anion Topologies

For topological analysis, the theory of graphical (nodal) representation of crystal structures [16] and the anion topology method [17] were used along with the classification suggested in [18]. Anion topologies were used to describe the layered complexes having edge-sharing polymerization of uranyl coordination polyhedra. For the rest of the structures, graphical representation was used. Each graph has a special index $ccD\text{--}U\text{:}Se\text{--}\#$, where *cc* means “cation-centered”, *D* indicates dimensionality (1—chains; and 2—sheets), *U:Se* ratio, *#* is the registration number of the unit. Each anion topology is indicated by a, so called, ring symbol, $p_1^{r_1} p_2^{r_2} \dots$, where *p* is the sum of vertices in a topological cycle, and *r* is the number of the respective cycles in the reduced section of the layer.

Three-connected selenate tetrahedra, sharing three of its corners with adjacent uranyl bipyramids, and 2- or 3-connected selenite pyramids, can possess the fourth non-shared corner or lone electron pair, respectively, oriented either *up*, *down*, or disordered relative to the plane of the chain, layer, or, in particular, to the equatorial plane of the uranyl bipyramid. Such ambiguity gives rise to geometric isomerism with various orientations of the Se-centered polyhedra. To distinguish the isomers, their orientation matrices were assigned using symbols **u** (*up*), **d** (*down*), **m** (orientation *up-down* topologically equivalent), or \square (white vertex, Se-centered polyhedron, is missing in the graph).

2.5. Complexity Calculations

In order to characterize and quantify the impact of each substructural units on the formation of a particular architecture, the structural complexity approach recently developed by S.V. Krivovichev [19–23], which allows comparison of the structures in terms of their information content, was used.

The complexity of the crystal structure was estimated as a Shannon information content per atom (I_G) and per unit cell ($I_{G,\text{total}}$) using the following equations:

$$I_G = - \sum_{i=1}^k p_i \log_2 p_i \quad (\text{bits/atom}), \quad (1)$$

$$I_{G,total} = -v I_G = -v \sum_{i=1}^k p_i \log_2 p_i \quad (\text{bits/cell}), \quad (2)$$

where k is the number of different crystallographic orbits (independent sites) in the structure and p_i is the random choice probability for an atom from the i -th crystallographic orbit, that is:

$$p_i = m_i/v, \quad (3)$$

where m_i is a multiplicity of a crystallographic orbit (i.e., the number of atoms of a specific Wyckoff site in the reduced unit cell), and v is the total number of atoms in the reduced unit cell.

The reliable correlation of structural complexity parameters is possible only for compounds with the same or very close chemical composition (e.g., polymorphs), whereas changes in the hydration state, nature of interstitial complexes, and size and shape of organic molecules could significantly affect the overall complexity behavior. In this light, within the current crystal chemical review, structural complexity parameters of various building blocks (uranyl selenite units, interstitial structure, H-bonding system) were calculated to analyze their contributions to the complexity of the whole structure. This approach suggested by S.V. Krivovichev [24] and recently successfully implemented in [25,26] allows the factors that influence the symmetry preservation or reduction of uranyl selenite units to be revealed, and it shows which of the multiple blocks plays the most important role in a particular structure formation.

3. Results

3.1. Uranyl Selenite Minerals

Guilleminite, $\text{Ba}[(\text{UO}_2)_3(\text{SeO}_3)_2\text{O}_2](\text{H}_2\text{O})_3$ [1,27], and demesmaekerite, $\text{Pb}_2\text{Cu}_5[(\text{UO}_2)_2(\text{SeO}_3)_6(\text{OH})_6](\text{H}_2\text{O})_2$ [2,28], were the first uranyl selenites found in nature (Table 1). These minerals occur in the lower part of the oxidized zone of the copper-cobalt deposit of Musonoi (Katanga, DR Congo). The first mineral was named after the general director of the Union Minière du Haut-Katanga (UMHK), co-founder of the International Mineralogical Association, French chemist and mineralogist, Jean-Claude Guillemin. Guilleminite crystallizes in the orthorhombic $Pmn2_1$ space group and forms small tabular crystals and canary yellow crusts. It occurs in association with malachite, uranophane- α , wulfenite, etc. The second mineral was named in honor of the director of the geological department of the UMHK, Belgian geologist Gaston Demesmaeker. Demesmaekerite crystallizes in the triclinic $P-1$ space group in the form of lamellar and elongated crystals of bottle-green to dark olive-green color in association with malachite, uranophane- α , chalcocite, and other uranyl-selenites: Namely marthozite and derriksite as well as guilleminite.

Marthozite, $\text{Cu}[(\text{UO}_2)_3(\text{SeO}_3)_2\text{O}_2](\text{H}_2\text{O})_8$ [3,29], was also found in the Musonoi mine within a few years after, and named to honor Aimé Marthoz, former director of the UMHK. Marthozite crystallizes in the orthorhombic $Pbn2_1$ space group, in the form of well-faceted green crystals, in association with the other selenites, including guilleminite and demesmaekerite, as well as kasolite, cuprosklodowskite, malachite, chalcocite, and sengierite. Mineral is isotypic with guilleminite.

A few years later, derriksite, $\text{Cu}_4[(\text{UO}_2)(\text{SeO}_3)_2](\text{OH})_6$ [4,30], was found at the same deposit in Congo, and named after Jean-Marie François Joseph Derriks, a Belgian geologist and administrator of the UMHK. Derriksite crystallizes in the orthorhombic $Pn2_1m$ space group, as sub-green up to bottle-green-colored crystals, elongated at [001] or incrustations and fine-crystalline crusts on digenite and the mineral is associated with marthozite, demesmaekerite, kasolite, malachite, etc.

Table 1. Crystallographic characteristics of natural uranyl selenites.

No.	Formula/Mineral Name	Topology	Sp. Gr.	a , Å/ α , °	b , Å/ β , °	c , Å/ γ , °	Reference
Chains							
1	$\text{Cu}_4[(\text{UO}_2)(\text{SeO}_3)_2](\text{OH})_6$ derriksite	cc1–1:2–1	$Pn2_1m$	5.570(2)/90	19.088(8)/90	5.965(2)/90	[2]
2	$\text{Pb}_2\text{Cu}_5[(\text{UO}_2)_2(\text{SeO}_3)_6(\text{OH})_6](\text{H}_2\text{O})_2$ demesmaekerite	cc1–1:3–2	$P-1$	11.9663(9)/89.891(8)	10.0615(14)/100.341(11)	5.6318(8)/91.339(9)	This work, [4]
Layers with edge-linkage							
3	$\text{Cu}[(\text{UO}_2)_3(\text{SeO}_3)_2\text{O}_2](\text{H}_2\text{O})_8$ marthozite	$6^15^24^23^2$	$Pbn2_1$	6.9879(4)/90	16.454(1)/90	17.223(1)/90	[17]
4	$\text{Ba}[(\text{UO}_2)_3(\text{SeO}_3)_2\text{O}_2](\text{H}_2\text{O})_4$ guilleminite		$Pmn2_1$	16.762(1)/90	7.2522(5)/90	7.0629(4)/90	This work, [18]
5	$\text{Na}(\text{H}_3\text{O})[(\text{UO}_2)_3(\text{SeO}_3)_2\text{O}_2](\text{H}_2\text{O})_4$ larisaite		$P11m$	6.9806(9)/90	7.646(1)/90	17.249(2)/90.039(4)	[19]
6	$[(\text{UO}_2)_3(\text{SeO}_3)_2(\text{OH})_2](\text{H}_2\text{O})_5$ haynesite		$Pnc2$ or $Pncm$	6.935/90	8.025/90	17.430/90	[21]
7	$\text{Ca}[(\text{UO}_2)_3(\text{SeO}_3)_2(\text{OH})_4](\text{H}_2\text{O})_4$ piretite		$Pmn2_1$ or $Pmmm$	7.010(3)/90	17.135(7)/90	17.606(4)/90	[22]

Next, natural uranyl selenite was discovered in 20 years across the Atlantic, in the Repete mine (Utah, USA). Haynesite, $[(\text{UO}_2)_3(\text{SeO}_3)_2(\text{OH})_2](\text{H}_2\text{O})_5$ [5,31,32] is named after the American geologist Patrick Eugene Haynes. Haynesite is orthorhombic, occurs as amber-yellow tablets, transparent to translucent, elongated at [001], and as acicular prismatic rosettes up to 3 mm in diameter, and is associated with andersonite, boltwoodite, gypsum, and calcite as crusts on mudstones and sandstones.

Piretite, $\text{Ca}(\text{UO}_2)_3(\text{SeO}_3)_2(\text{OH})_4 \cdot 4\text{H}_2\text{O}$ [6], calcium uranyl selenite from Shinkolobwe mine (Katanga, DR Congo) is named after the Belgian crystallographer Paul Piret. Piretite is orthorhombic, it crystallizes as lemon-yellow elongated tablets, irregular in outline and up to 3 mm, flattened on (001), or as needle-prismatic crystals up to 5 mm. It occurs in association with a masuyite-like uranyl-lead oxide as crusts on uraninite. It should be noted that crystal structures of haynesite and piretite have still not been determined.

The last to date, uranyl selenite mineral, larisaite, $\text{Na}(\text{H}_3\text{O})[(\text{UO}_2)_3(\text{SeO}_3)_2\text{O}_2](\text{H}_2\text{O})_4$ [7], was found in the Repete mine (Utah, UT, USA) and named in honor of Larisa Nikolaevna Belova, a Russian mineralogist and crystallographer who made a significant contribution to the knowledge on uranium minerals. Larisaite occurs as canary-yellow lamellar crystals up to 1 mm long, and as radial aggregates up to 2 mm across; most crystals are fissured and ribbed. The mineral is a supergene product associated with calcite, quartz, gypsum, montmorillonite, wölsendorfite, andersonite, haynesite, and uranophane- α in sedimentary rocks.

3.2. Synthetic Uranyl Compounds with Selenite Ions

The first synthetic and the simplest uranyl selenite, $[(\text{UO}_2)(\text{SeO}_3)]$, was obtained in 1978 [33] (and its neptunyl analog has been recently reported [34] as well). Further, the research undertaken by V. E. Mistryukov and Yu. N. Mikhailov from the Kurnakov Institute of General and Inorganic Chemistry RAS (Russian Federation), and by V.N. Serezhkin and L.B. Serezhkina from the Samara State University (Russian Federation) should be mentioned, who studied uranyl selenites with electroneutral ligands and the first Na-bearing synthetic uranyl selenite compounds. Nearly half of the synthetic compounds described within this review were synthesized and characterized by T.E. Albrecht-Schmitt and co-workers (Table 2). The significant impact of their works on the development of uranyl selenites' structural chemistry should be especially noted.

Synthetic compounds, whose structures are based on inorganic units with the linkage of *Ur* to selenite oxyanions (Table 2), could be divided into two groups: Pure inorganic and organically templated phases.

Table 2. Crystallographic characteristics of synthetic uranyl selenites and selenite-selenates.

No.	Formula	Topology	Sp. Gr.	<i>a</i> , Å/α, °	<i>b</i> , Å/β, °	<i>c</i> , Å/γ, °	Reference
Chains							
8	[(UO ₂)(HSeO ₃) ₂ (H ₂ O)]	cc1–1:2–1	<i>A2/a</i>	6.354(1)/90	12.578(2)/82.35(1)	9.972(2)/90	[35]
9	[(UO ₂)(HSeO ₃) ₂](H ₂ O)		<i>C2/c</i>	9.924(5)/90	12.546(5)/98.090(5)	6.324(5)/90	[36]
10	Ca[(UO ₂)(SeO ₃) ₂]	cc1–1:2–14	<i>P</i> –1	5.5502(6)/104.055(2)	6.6415(7)/93.342(2)	11.013(1)/110.589(2)	[37]
11	Sr[(UO ₂)(SeO ₃) ₂]		<i>P</i> –1	5.6722(4)/104.698(1)	6.7627(5)/93.708(1)	11.2622(8)/109.489(1)	[38]
12	Sr[(UO ₂)(SeO ₃) ₂](H ₂ O) ₂	cc1–1:2–15	<i>P</i> –1	7.0545(5)/106.995(1)	7.4656(5)/108.028(1)	10.0484(6)/98.875(1)	[37]
13	Na ₃ [H ₃ O][[(UO ₂)(SeO ₃) ₂] ₂ (H ₂ O)]		<i>P</i> –1	9.543(6)/66.69(2)	9.602(7)/84.10(2)	11.742(8)/63.69(1)	[39]
Layers with corner-linkage							
14	[NH ₄] ₂ [(UO ₂)(SeO ₃) ₂](H ₂ O) _{0.5}	cc2–1:2–4	<i>P</i> ₂₁ / <i>c</i>	7.193(5)/90	10.368(5)/91.470(5)	13.823(5)/90	[36]
15	[NH ₄][[(UO ₂)(SeO ₃)(HSeO ₃)]		<i>P</i> ₂₁ / <i>n</i>	8.348(2)/90	10.326(2)/97.06(2)	9.929(2)/90	[40]
16	K[(UO ₂)(HSeO ₃)(SeO ₃)]		<i>P</i> ₂₁ / <i>n</i>	8.4164(4)/90	10.1435(5)/97.556(1)	9.6913(5)/90	[41]
17	Rb[(UO ₂)(HSeO ₃)(SeO ₃)]		<i>P</i> ₂₁ / <i>n</i>	8.4167(5)/90	10.2581(6)/96.825(1)	9.8542(5)/90	[41]
18	Cs[(UO ₂)(HSeO ₃)(SeO ₃)]		<i>P</i> ₂₁ / <i>c</i>	13.8529(7)/90	10.6153(6)/101.094(1)	12.5921(7)/90	[41,42]
19	Cs[((U,Np)O ₂)(HSeO ₃)(SeO ₃)]		<i>P</i> ₂₁ / <i>n</i>	8.4966(2)/90	10.3910(3)/93.693(1)	10.2087(3)/90	[42]
20	Tl[(UO ₂)(HSeO ₃)(SeO ₃)]		<i>P</i> ₂₁ / <i>n</i>	8.364(3)/90	10.346(4)/97.269(8)	9.834(4)/90	[41]
21	Cs[(UO ₂)(SeO ₃)(HSeO ₃)](H ₂ O) ₃		<i>P</i> ₂₁ / <i>n</i>	8.673(2)/90	10.452(3)/105.147(4)	13.235(4)/90	[43]
22	Na[(UO ₂)(SeO ₃)(HSeO ₃)](H ₂ O) ₄		<i>P</i> ₂₁ / <i>n</i>	8.8032(5)/90	10.4610(7)/105.054(2)	13.1312(7)/90	[44]
23	[H ₃ O][[(UO ₂)(SeO ₄)(HSeO ₃)]		<i>P</i> ₂₁ / <i>n</i>	8.668(2)/90	10.655(2)/97.88(2)	9.846(2)/90	[45]
24	Ag ₂ [(UO ₂)(SeO ₃) ₂]	cc2–1:2–5	<i>P</i> ₂₁ / <i>n</i>	5.8555(6)/90	6.5051(7)/96.796(2)	21.164(2)/90	[41]
Layers with edge-linkage							
25	Pb[(UO ₂)(SeO ₃) ₂]	cc2–1:2–19	<i>Pmc</i> ₂₁	11.9911(7)/90	5.7814(3)/90	11.2525(6)/90	[41]
26	Ba[(UO ₂)(SeO ₃) ₂]	cc2–1:2–21	<i>P</i> ₂₁ / <i>c</i>	7.3067(6)/90	8.1239(7)/100.375(2)	13.651(1)/90	[37]
27	[(UO ₂)(SeO ₃)]	6 ¹ 3 ²	<i>P</i> ₂₁ / <i>m</i>	5.408(2)/90	9.278(1)/93.45(10)	4.254(1)/90	[33]
28	Sr[(UO ₂) ₃ (SeO ₃) ₂ O ₂](H ₂ O) ₄	6 ¹ 5 ² 4 ² 3 ²	<i>C</i> ₂ / <i>m</i>	17.014(2)/90	7.0637(7)/100.544(2)	7.1084(7)/90	[38]
29	Li ₂ [(UO ₂) ₃ (SeO ₃) ₂ O ₂](H ₂ O) ₆		<i>P</i> ₂₁ / <i>c</i>	7.5213(9)/90	7.0071(8)/98.834(2)	17.328(2)/90	[46]
30	Cs ₂ [(UO ₂) ₄ (SeO ₃) ₅](H ₂ O) ₂	6 ¹ 5 ³ 4 ⁶ 3 ⁵	<i>P</i> ₂₁ / <i>n</i>	10.913(3)/90	12.427(3)/90.393(3)	18.448(4)/90	[46]
31	Cs ₂ [(UO ₂) ₇ (SeO ₄) ₂ (SeO ₃) ₂ (OH) ₄ O ₂](H ₂ O) ₅	6 ¹ 5 ⁶ 4 ⁶ 3 ⁶	<i>P</i> ₂₁ / <i>m</i>	9.1381(3)/90	15.0098(5)/91.171(1)	15.1732(5)/90	[46]
32	UO ₂ Se ₂ O ₅	8 ¹ 5 ² 3 ⁸	<i>P</i> –1	9.405(2)/93.01(3)	11.574(2)/93.66(3)	6.698(2)/109.69(1)	[47]

Table 2. Cont.

No.	Formula	Topology	Sp. Gr.	a , Å/ α , °	b , Å/ β , °	c , Å/ γ , °	Reference
Organically templated							
33	$[\text{C}_4\text{H}_{12}\text{N}][(\text{UO}_2)(\text{SeO}_3)(\text{NO}_3)]$	cc1–1:2–12	$C2/m$	21.888(3)/90	6.950(1)/97.618(3)	8.350(1)/90	[48]
34	$[\text{C}_6\text{H}_{14}\text{N}_2]_{0.5}[(\text{UO}_2)(\text{HSeO}_3)(\text{SeO}_3)(\text{H}_2\text{O})_{0.5}(\text{CH}_3\text{CO}_2\text{H})_{0.5}]$	cc2–1:2–4	$Pnma$	13.086(1)/90	17.555(1)/90	10.5984(7)/90	[49]
35	$[\text{C}_4\text{H}_{12}\text{N}_2]_{0.5}[(\text{UO}_2)(\text{HSeO}_3)(\text{SeO}_3)]$		$P2_1/c$	10.9378(5)/90	8.6903(4)/90.3040(8)	9.9913(5)/90	[49]
36	$[(\text{C}_2\text{H}_8\text{N}_2)\text{H}_2][(\text{UO}_2)(\text{SeO}_3)(\text{HSeO}_3)](\text{NO}_3)(\text{H}_2\text{O})_{0.5}$		$Pbca$	13.170(3)/90	11.055(2)/90	18.009(4)/90	[50]
37	$[\text{C}_5\text{H}_{14}\text{N}][(\text{UO}_2)(\text{SeO}_4)(\text{HSeO}_3)]$		$P2_1/n$	11.553(2)/90	10.645(2)/108.05(2)	12.138(2)/90	[51]
38	$[\text{C}_2\text{H}_8\text{N}][(\text{UO}_2)(\text{SeO}_4)(\text{HSeO}_3)]$		$P2_1/n$	8.475(3)/90	12.264(2)/95.23(3)	10.404(3)/90	[52]
39	$[\text{C}_5\text{H}_6\text{N}][(\text{UO}_2)(\text{SeO}_4)(\text{HSeO}_3)]$		$P2_1/n$	8.993(3)/90	13.399(5)/108.230(4)	10.640(4)/90	[53]
40	$[\text{C}_9\text{H}_{24}\text{N}_2][(\text{UO}_2)(\text{SeO}_4)(\text{HSeO}_3)](\text{NO}_3)$		$P-1$	10.748(1)/109.960(1)	13.885(1)/103.212(2)	14.636(1)/90.409(1)	[54]
41	$[\text{C}_2\text{H}_8\text{N}][(\text{H}_5\text{O}_2)(\text{H}_2\text{O})][(\text{UO}_2)_2(\text{SeO}_4)_3(\text{H}_2\text{SeO}_3)](\text{H}_2\text{O})$	cc2–1:2–14	$P2_1/n$	14.798(1)/90	10.024(1)/111.628(1)	16.418(1)/90	[55]
42	$[\text{C}_4\text{H}_{15}\text{N}_3][\text{H}_3\text{O}]_{0.5}[(\text{UO}_2)_2(\text{SeO}_4)_{2.93}(\text{SeO}_3)_{0.07}(\text{H}_2\text{O})](\text{NO}_3)_{0.5}$	cc2–2:3–4	$P2_1/c$	11.1679(4)/90	10.9040(4)/98.019(1)	17.991(1)/90	[56]
43	$[\text{C}_5\text{H}_{14}\text{N}]_4[(\text{UO}_2)_3(\text{SeO}_4)_4(\text{HSeO}_3)(\text{H}_2\text{O})](\text{H}_2\text{SeO}_3)(\text{HSeO}_4)$	cc2–3:5–3	$P-1$	11.707(1)/73.90(1)	14.817(1)/76.22(1)	16.977(2)/89.36(1)	[57]
44	$[\text{C}_2\text{H}_8\text{N}]_3(\text{C}_2\text{H}_7\text{N})[(\text{UO}_2)_3(\text{SeO}_4)_4(\text{HSeO}_3)(\text{H}_2\text{O})]$		$Pnma$	11.659(1)/90	14.956(2)/90	22.194(2)/90	[56]
45	$[\text{C}_2\text{H}_8\text{N}]_2[\text{H}_3\text{O}][(\text{UO}_2)_3(\text{SeO}_4)_4(\text{HSeO}_3)(\text{H}_2\text{O})](\text{H}_2\text{SeO}_3)_{0.2}$		$P2_1/m$	8.3116(4)/90	18.636(1)/97.582(1)	11.5623(5)/90	[56]
46	$[\text{C}_8\text{H}_{15}\text{N}_2]_2[(\text{UO}_2)_4(\text{SeO}_3)_5]$	$6^15^34^63^5$	$Pnma$	18.860(2)/90	18.010(2)/90	11.140(1)/90	[58]

Most of the inorganic uranyl selenites were obtained during low or medium temperature hydrothermal experiments in the temperature range of 100 to 220 °C using Teflon-lined steel autoclaves. Various reagents were used as the source of uranium (U(VI) oxide, uranyl hydroxide, uranyl nitrate hexahydrate, uranyl acetate dihydrate), whereas selenous acid (H_2SeO_3) was the only source of Se(IV). To be precise, either acid itself or SeO_2 were used in the reactions, but Se(IV) dioxide reacts with water to form selenous acid. H_2SeO_3 is a very weak acid and it hardly dissociates at room temperature, which explains the required heating for the reaction. Several compounds obtained in different ways should be mentioned separately. Compounds **22** [44] and **23** [45] were obtained during evaporation at room temperature. The first compound was obtained from the reaction of $\text{UO}_2(\text{NO}_3)_2 \cdot 6\text{H}_2\text{O}$ with selenic acid (H_2SeO_4) in aqueous medium for 1 year, which could be explained by the reduction of Se(VI) to Se(IV) in the solution during the experiment. Moreover, as it was recently shown, the hydronium ions usually enter the structure at the very latest crystallization stages, when there are no more other cations in the solution [52,59,60]. The Na-bearing compound was obtained in the presence of sodium oxalate, which probably could be regarded as a catalyst of the uranyl selenite crystallization process. Another five compounds, **11** [38], **21** [43], **27** [33], **28** [38], and **32** [47], were obtained in the gas–solid or hydrothermal reactions using sealed tubes. In the case of the last three compounds, the temperature reached over 425 °C.

The majority of the organically templated compounds are actually uranyl selenites-selenates. The selenite anions that are arranged in the structures of such compounds are in minor amounts with respect to the selenate groups. Such a tendency comes from the experimental conditions, in which the source of Se was the selenic acid. Selenic acid is less stable in environmental conditions than selenous acid, and it reduces to the latter during storage. Initially, pure H_2SeO_4 reagent after a few months of storage contains significant amount of $[\text{SeO}_3]^{2-}$ and $[\text{HSeO}_3]^-$ ions, which participate in the structure formation along with $[\text{SeO}_4]^{2-}$ groups. There are only five structures of organically templated uranyl selenites known without $[\text{SeO}_4]^{2-}$ oxyanions (Table 2), three of which (**34** [49], **35** [49], and **46** [58]) were obtained during mild hydrothermal experiments (130–150 °C) when the source of Se was again selenic acid. Here, the temperature and amine molecules or ionic liquids [58] acted as a reduction agent for H_2SeO_4 , since it is known that the selenic acid is easily reduced to $\text{H}_2\text{Se}^{4+}\text{O}_3$ and oxygen upon heating above 160 °C [61]. The other two organically templated uranyl selenites (**33** [48] and **36** [50]) were obtained during evaporation at room temperature from the aqueous solution of $\text{UO}_2(\text{NO}_3)_2 \cdot 6\text{H}_2\text{O}$, SeO_2 , and respective amine. Since SeO_2 transforms to weak selenous acid in water, the low dissociation ability of the latter [62] and the presence of $[\text{NO}_3]^-$ groups in the structures of both compounds explains the long crystallization process of 1 to 2 months. It is likely that dissociation of uranyl nitrate and the presence of amine finally helped to create an environment sufficient for the selenous acid dissociation, and thus to start the crystallization of uranyl selenites. Nitrate groups, in these cases, act as additional oxyanions involved in structure formation with a shortage of $[\text{SeO}_3]^{2-}$ groups.

3.3. Topological Analysis

The vast majority of the uranyl selenite crystal structures are based on the layered complexes of various topologies (Tables 1 and 2), and only nine compounds have chain-based crystal structures. However, among those nine compounds, two are uranyl selenite minerals.

Crystal structures of derriksite and another two synthetic compounds (Tables 1 and 2, Figure 1a–c), which are actually the same but were refined in different space groups, are based on the 1D units of the $cc1-1:2-1$ topological type (graph is an infinite chain of four-membered vertex-sharing rings). The graph corresponds to the type of chains, which were observed in the kröhnkite [63]. This topology is one of the most common and simplest chain topologies among U(VI)-bearing compounds with the $[\text{TO}_m]^{n-}$ groups ($m = 3, 4$; $T = \text{S, Se, P, As}$). It was observed in the structures of uranyl-sulfate minerals as svornostite, $\text{K}_2\text{Mg}[(\text{UO}_2)(\text{SO}_4)_2]_2(\text{H}_2\text{O})_8$ [64], rietveldite, $\text{Fe}(\text{UO}_2)(\text{SO}_4)_2(\text{H}_2\text{O})_5$ [65], and their Mg-bearing synthetic analogues $\text{Mg}[(\text{UO}_2)(\text{TO}_4)_2(\text{H}_2\text{O})](\text{H}_2\text{O})_4$ ($T = \text{S, Se}$) [66]. Although the topology of chains is the same, their structures are remarkably different, representing two different isomers.

In the case of derriksite (Figure 1c), U^{6+} atoms present in the tetragonal bipyramidal coordination, where all four equatorial O atoms are shared with the $[SeO_3]^{2-}$ groups, and each selenite group in turn has only two O atoms shared with two neighbors' *Ur*. Uranyl selenite chains in the structure of derriksite are directed along [001] and the equatorial planes of uranyl bipyramids are arranged parallel to the (101). In between the chains, Cu-centered tri-octahedral layers are observed as being arranged parallel to (010), in which each Cu atom has four OH^- groups shared with the neighbor Cu atoms and two more vertices in the *trans*-orientation are the third vertices of selenite pyramids, non-shared with U-centered bipyramids. Selenite groups are arranged in such a way that lone electron pairs from one side of the U-Se chain are directed in one way, and from the other side, in the opposite direction (*up* or *down*), relative to the equatorial planes of uranyl bipyramids. Thus, the sequence of orientation symbols could be written as (u)(d). The latter has been termed an *orientation matrix*. In the structures of synthetic $[(UO_2)(HSeO_3)_2(H_2O)]$ [35,36] compounds, U^{6+} atoms are arranged in the center of pentagonal bipyramids, in which four equatorial O atoms are shared with the $[HSeO_3]^-$ groups and the fifth vertex is occupied by the H_2O molecule. Hydrogen selenite groups also have two O atoms shared with two neighboring *Ur* and the third vertex is attributed to the OH^- group. The linkage of chains into the 3D structure is carried out by the means of H-bonding between the neighbor chains only. The arrangement of lone electron pairs relative to the equatorial planes of uranyl bipyramids is staggered on both sides of the chain, so the orientation matrix for the current geometrical isomer is (ud)(du).

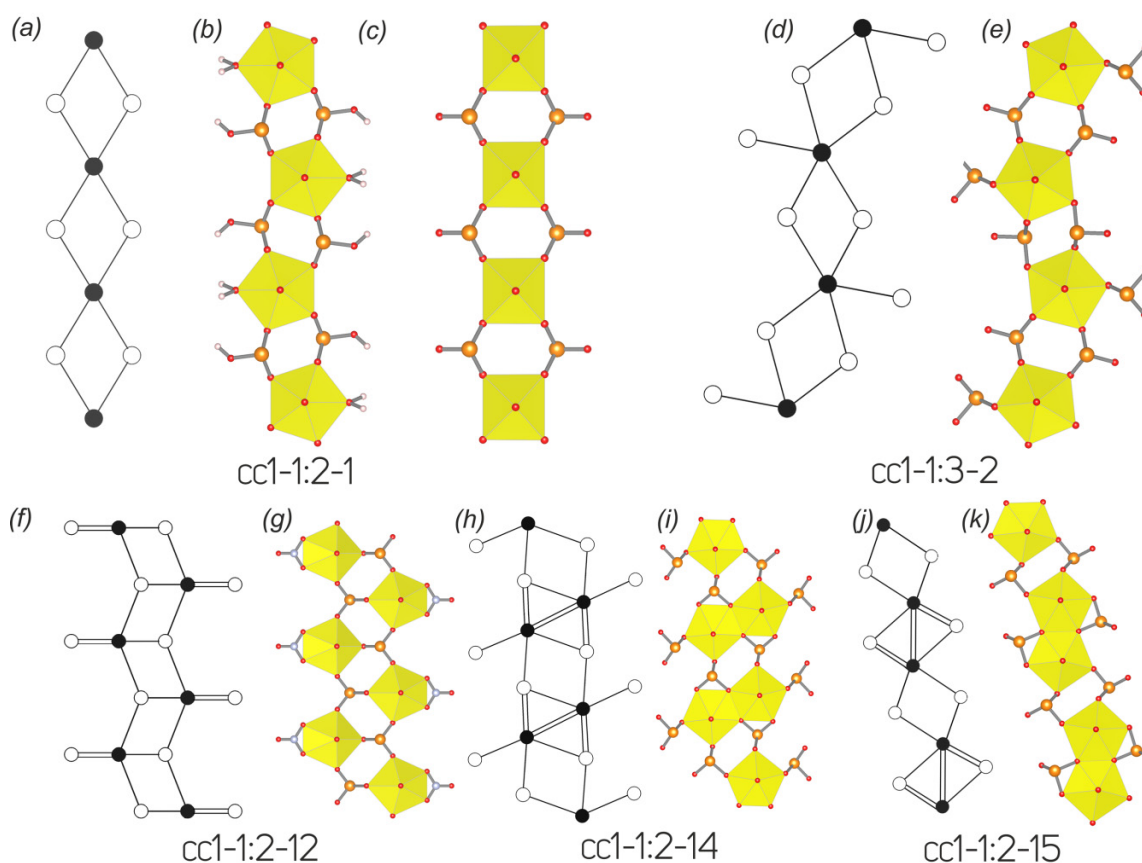


Figure 1. (a–k) 1D complexes in the crystal structures of natural and synthetic uranyl selenites (a–k: see text for details). Legend: U-bearing coordination polyhedra = yellow; Se atoms = orange; O atoms = red; H atoms = white; N atoms = light blue; black nodes = U atoms, white nodes = Se atoms. $Se^{IV}O_3$ trigonal pyramids and NO_3 groups are shown in a ball-and-stick mode.

The crystal structure of demesmaekerite is based on the chains of the *cc1-1:3-2* topology (Figure 1d,e), which is very similar to the previous type. The graph is a vertex-sharing infinite chain of

four-membered rings with additional one-connected selenite group to each *Ur*. This topology is quite rare and has been observed in the structures of two synthetic uranyl chromates $\text{Na}_4[(\text{UO}_2)(\text{CrO}_4)_3]$ [67] and $\text{K}_5[(\text{UO}_2)(\text{CrO}_4)_3](\text{NO}_3)(\text{H}_2\text{O})_3$ [68], two uranyl molybdates $\text{Na}_3\text{Ti}_5[(\text{UO}_2)(\text{MoO}_4)_3]_2(\text{H}_2\text{O})_3$ and $\text{Na}_{13}\text{Ti}_3[(\text{UO}_2)(\text{MoO}_4)_3]_4(\text{H}_2\text{O})_5$ [69], and one uranyl selenate $(\text{C}_2\text{H}_8\text{N})_3[(\text{UO}_2)(\text{SeO}_4)_2(\text{HSeO}_4)]$ [52]. U^{6+} atoms are arranged in the centers of pentagonal bipyramids, so that four equatorial vertices of which are shared with two-connected selenite groups (as in previous type), and the fifth vertex that was occupied by H_2O molecule, now is replaced by another one-connected $[\text{SeO}_3]^{2-}$ pyramid. Uranyl selenite chains are passing along the (101), and stacked one above the other, forming blocks parallel to (010). These blocks are separated by the sheets of edge-shared Cu- and Pb-centered coordination polyhedra. There are three types of Cu^{2+} -centered octahedra in the structure of demesmaekerite, $[\text{CuO}_4(\text{OH})_2]^{8-}$, $[\text{CuO}_3(\text{OH})_3]^{7-}$, and $[\text{CuO}_2(\text{OH})_3(\text{H}_2\text{O})]^{6-}$, and the single type of ninefold $[\text{Pb}^{2+}\text{O}_6(\text{OH})_3]^{13-}$ complexes. Lone electron pairs of one- and two-connected selenite groups from one side of the U-Se chain are oriented in the same direction, while on the other side the direction is the opposite, thus the orientation matrix could be written as **(u)(d)**.

The crystal structure of the organically templated compound **33** [48] is based on the uranyl selenite nitrate 1D complexes that belong to the *cc1-1:2-12* topological type (Figure 1f,g). This topology has been observed in the structures of several uranyl and neptunyl sulfates and selenates, for example, see [70–73], and represents an infinite chain of edge-shared four-membered cycles, in which each uranyl polyhedron has three equatorial vertices shared with three selenite groups while the left pair of O atoms is edge-shared with the $[\text{NO}_3]^-$ group. Being three-connected to the neighbor *Ur*, $[\text{SeO}_3]^{2-}$ pyramids have a lone electron pair oriented either *up* or *down* relative to the equatorial planes of uranyl bipyramids in the **(ud)** $_{\infty}$ sequence.

The crystal structures of Ca- [37] and Sr-bearing [38] isotopic uranyl selenites are based on 1D complexes of the *cc1-1:2-14* topological type (Figure 1h,i), which are built by the dimers of edge-sharing uranyl pentagonal bipyramids that are interlinked by the pair of edge- and vertex-sharing selenite groups with another one-connected selenite group decorating the fifth non-shared equatorial vertices of U polyhedra from both sides of such a double-wide chain. It should be noted that $[\text{SeO}_3]^{2-}$ pyramids, which are involved in the linkage of U dimers, have lone electron pairs oriented *up* from one side of the chain, and *down* from the other side, thus illustrating the **(ud)** $_{\infty}$ sequence. This type of chains occurs in the structures of two uranyl minerals: Parsonite, $\text{Pb}_2[(\text{UO}_2)(\text{PO}_4)_2]$, [74] and hallmondite, $\text{Pb}_2[(\text{UO}_2)(\text{AsO}_4)_2](\text{H}_2\text{O})_n$, [75].

The crystal structures of two more Sr- [37] and Na-hydronium-bearing [39] compounds are based on the uranyl selenite chains with an edge-sharing motif, similar to the previous one. Chains belong to the *cc1-1:2-15* topological type (Figure 1j,k), and are built by the dimers of edge-sharing uranyl pentagonal bipyramids, which, in contrary to the aforementioned topology, are interlinked by a pair of only vertex-sharing selenite groups, while edge-sharing selenite pyramids in this case decorate both sides of the chain. Both compounds represent two different geometrical isomers, assuming the orientation of lone electron pairs. Thus, Sr uranyl selenite possesses the same **(ud)** $_{\infty}$ sequence, as in a previous case, while the Na-bearing compound has a **(u)** $_{\infty}$ sequence. This type of topology has been observed in several synthetic uranyl chromates, phosphates, and arsenates, as well as in lakebogaite, $\text{CaNa}(\text{Fe}^{3+})_2[(\text{H}(\text{UO}_2)_2(\text{PO}_4)_4(\text{OH})_2)(\text{H}_2\text{O})_8]$ [76].

The crystal structures of 17 synthetic uranyl selenites are based on the layers, which belong to the *cc2-1:2-4* topological type (Figure 2a,b), the most common among the uranyl selenite compounds and among the layered uranyl compounds, generally. The topology consists of dense four-membered cycles and large hollow eight-membered rings. It is worth noting, that almost all sheets of this topology contain protonated $[\text{HSeO}_3]^-$ groups with the H-bonds arranged inside the eight-membered cycles. Although the topology of the sheets remains the same, their real architecture is quite diverse, which occurs due to various blocks involved in the structure formation. Thus, the structures of these compounds are formed via combination of the $[\text{UO}_7]^{8-}$, $[\text{HSeO}_3]^-$, $[\text{SeO}_3]^{2-}$, and $[\text{SeO}_4]^{2-}$ coordination polyhedra through common oxygen atoms. Uranyl pentagonal bipyramids share all

of five equatorial O atoms with the selenite or selenate groups, while Se-bearing oxyanions act as two- or three-connected units. Such a diversity of building blocks opens up the possibility of a large number of geometric isomers' existence. Within the uranyl selenite and selenite-selenate compounds of *cc2-1:2-4* topology, three isomers are distinguished: Layers, containing only selenite groups; those, having selenite and hydrogen selenite groups; and those with hydrogen selenite groups and selenate tetrahedra. However, what is the most interesting, is that all three isomers have a similar orientation of lone electron pairs and fourth non-shared vertices (for tetrahedra), which is described by the very simple (**ud**) matrix. Only except for the compound **36**, which has the (**ud**)(**du**) matrix.

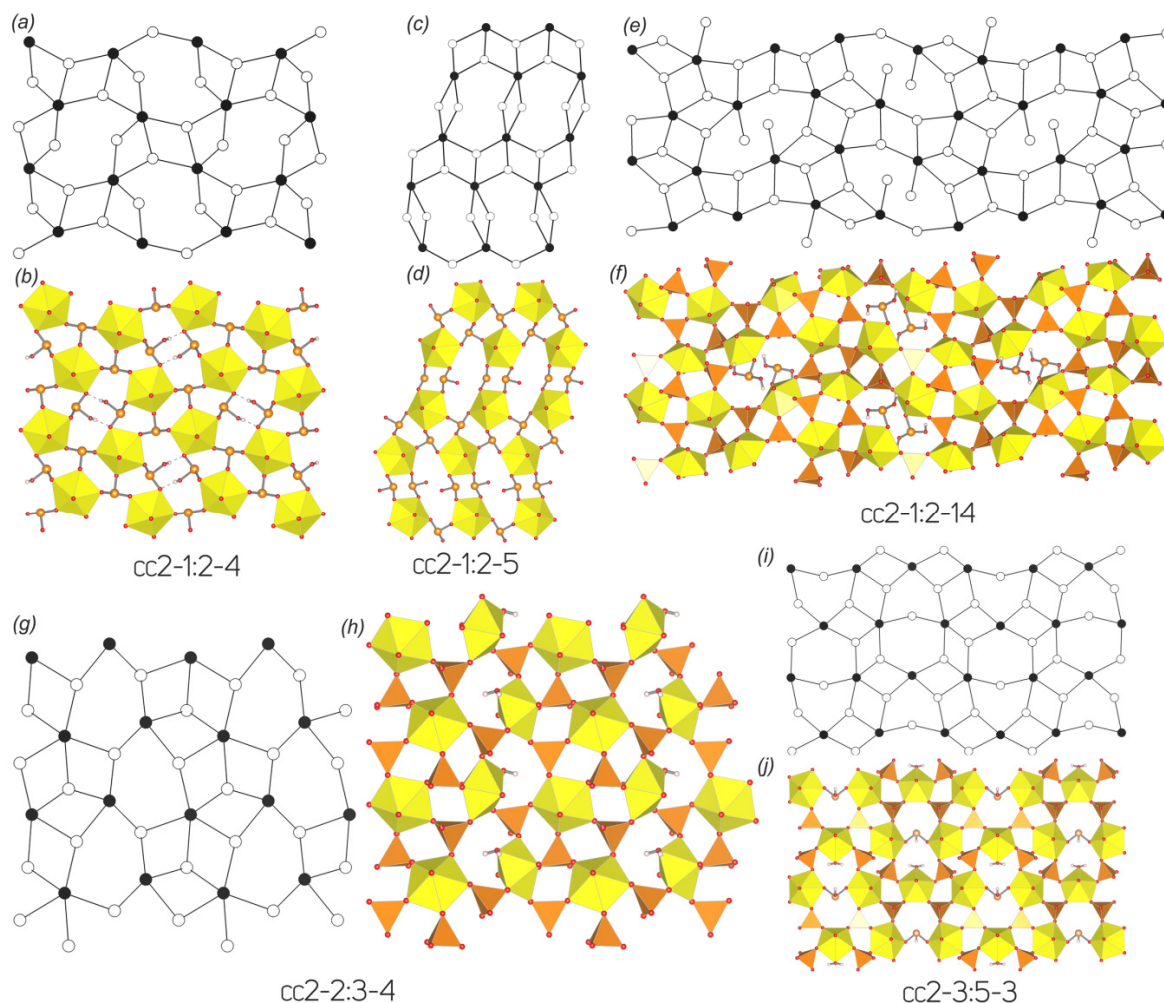


Figure 2. (a–j) 2D complexes based on corner-sharing linkage in the crystal structures of synthetic uranyl selenites and selenite-selenates (a–j: see text for details). Legend: see Figure 1; $\text{Se}^{\text{VI}}\text{O}_4$ groups = orange tetrahedra.

The crystal structures of Ag-bearing uranyl selenite [41] is based on the layered complex of *cc2-1:2-5* topological type (Figure 2c,d). This type of topology has been observed in the structures of several synthetic uranyl and neptunyl molybdates as $\text{Na}_2(\text{UO}_2)(\text{MoO}_4)_2$ [77] and $\text{K}_3\text{NpO}_2(\text{MoO}_4)_2$ [78]. Topological types *cc2-1:2-4* and *cc2-1:2-5* have nearly identical chemical composition and looks quite similar. Those graphs are built from the similar four- and eight-membered rings, and even have the same connectivity of black and white vertices (U and Se polyhedra, respectively), but the topologies are different due to differences in coordination sequence [18]. Such chemically identical, but topologically different structural units are called topological or structural isomers. It should be noted that the *cc2-1:2-4* topology is much more representative among the inorganic oxysalt compounds than

cc2-1:2-5. If the lone electron pair of the selenite pyramid would be equated to the fourth non-shared vertex of the selenate tetrahedron, the current isomer can be described by the (uddu)(dduu) matrix.

The crystal structure of **41** [55] is based on the 2D complexes, possessing unprecedented topology for both the structural chemistry of uranium and the chemistry of inorganic oxysalts in general, of the cc2-1:2-14 type (Figure 2e,f). U atoms are arranged in the centers of pentagonal bipyramids. Each $[\text{SeO}_4]^{2-}$ group is three-connected, coordinating three uranyl ions, whereas protonated selenite groups coordinate one uranyl ion each. The topology is remarkable due to the presence of one-connected branches inside eight-membered cycles, which are actually selenous acid groups.

The crystal structure of **25** [41] is based on the layered complexes of cc2-1:2-19 topological type (Figure 3a,b), which is a derivative of the autunite topology [18], where each uranyl pentagonal bipyramid has only one edge shared with the selenite group. The graph of the layer consists of eight-membered rings only. The current isomer can be described by the (uudd)(uddu)(dduu)(duud) matrix.

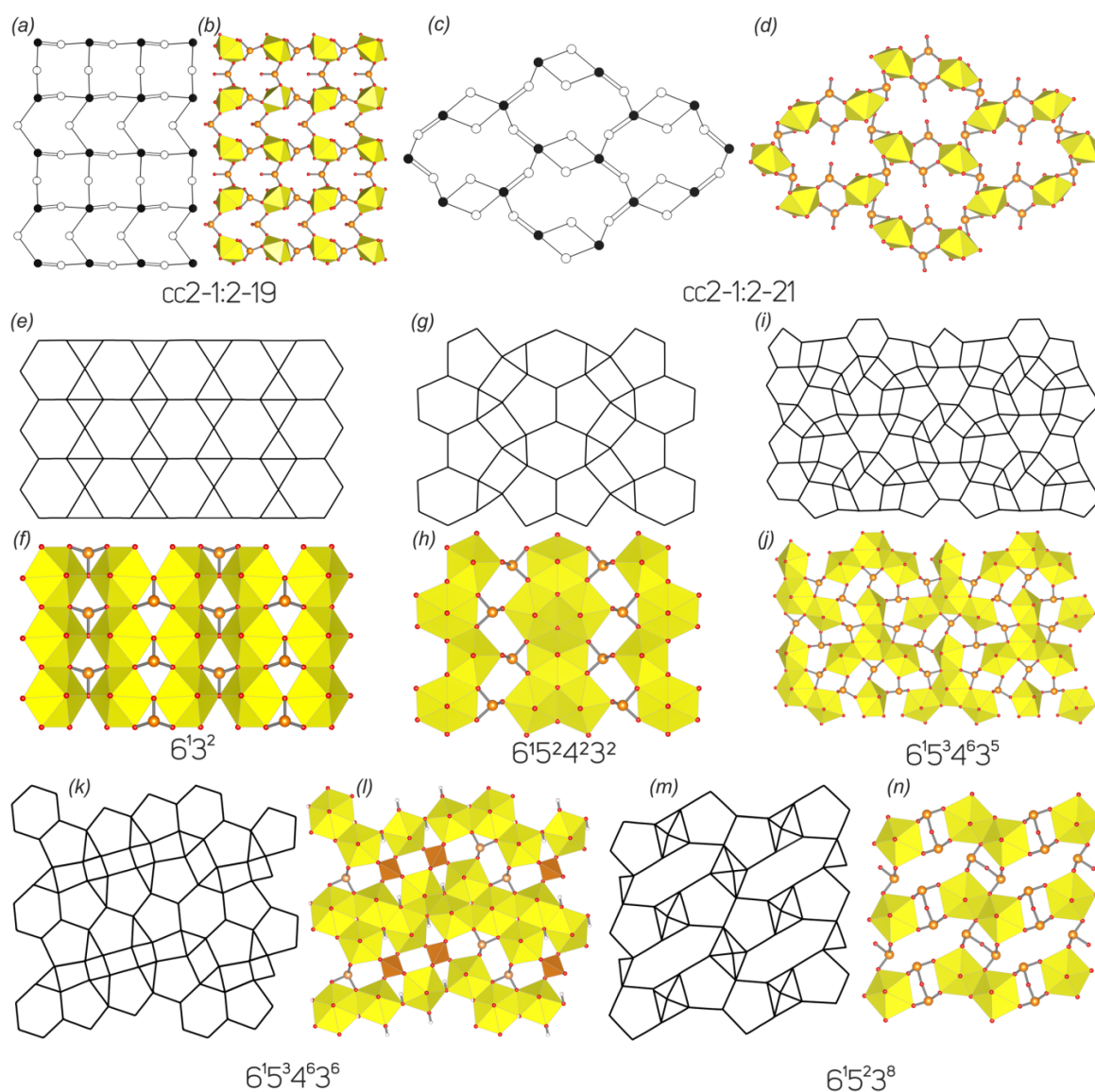


Figure 3. (a–n) 2D complexes based on edge-sharing linkage in the crystal structures of natural and synthetic uranyl selenites and selenite-selenates (a–n: see text for details). Legend: see Figures 1 and 2.

Compound **26** [37] is the only known uranyl selenite, which crystal structure is based on the layered complexes of cc2-1:2-21 topological type (Figure 3c,d). The graph of the U-bearing sheet

consists of dense 4-membered and large 12-membered rings. Double links between the black and white vertices in a graph indicate sharing of an edge between uranyl coordination polyhedra and the selenite pyramid. Despite the fact that $[\text{SeO}_3]^{2-}$ groups are two-connected, edge-sharing coordination generates a possibility for an orientational isomerism of the lone electron pair arrangement. Current isomer can be described by the (ud) matrix. It is of interest that interlayer Ba^{2+} cations are actually arranged within the layer, inside the 12-membered rings.

Next compound, **42** [56], got into the review with a large tolerance. There are three nonequivalent positions of Se in the structure, only one of which was occupied by both Se(VI) and Se(IV), and the amount of the latter is very small (~ 0.07 per formula unit). The current topology of the *cc2-2:3-4* type (Figure 2g,h) is one of the most common among synthetic uranyl sulfates, chromates, and selenates (>30 structures are known), but it has not been observed for any compound with a higher content of selenite ions than here.

The crystal structures of three organically templated compounds, **43** [57], **44**, and **45** [56], are based upon the layers with U:Se = 3:5 formed as a result of condensation of the $[\text{UO}_2]^{2+}$, $[\text{UO}_2(\text{H}_2\text{O})]^{2+}$, $[\text{Se}^{\text{VI}}\text{O}_4]^{2-}$, and $[\text{HSe}^{\text{IV}}\text{O}_3]^-$ coordination polyhedra by sharing common oxygen atoms. The corresponding graph of *cc2-3:5-3* topology is built by four- and six-membered rings (Figure 2i,j). This topology of inorganic complexes is typical for uranyl selenite-selenates but has also been observed in some pure uranyl selenates, for instance, $\text{Rb}_4[(\text{UO}_2)_3(\text{SeO}_4)_5(\text{H}_2\text{O})]$ [79]. The presence of two-connected selenite trigonal pyramids and three-connected selenate tetrahedra gives rise to geometric isomerism. Thus, the orientation matrices can be written as (ududud)(ud□du□) for the first and second, and (duuudd)(ud□du□) for the third compound, respectively.

The simplest uranyl selenite, at least from the chemical point of view, $[(\text{UO}_2)(\text{SeO}_3)]$ [33], has a layered structure (Figure 3e,f). According to Lussier et al. [80], the anionic topology of the layer of this compound belongs to the topology consisting of triangles and hexagons. The topology of the layer in this compound is the same as in mineral rutherfordine, $[(\text{UO}_2)(\text{CO}_3)]$ [81,82], which is why it is called a rutherfordine anion topology. This topology consists of parallel chains of edge-sharing hexagons divided by dimers of edge-sharing triangles. Each of the hexagons is occupied by Ur , and one triangle per dimer is occupied by the $[\text{SeO}_3]^{2-}$ group. The other half of the triangles is vacant. Electroneutral sheets are linked together by van der Waals interactions only. It should be noted that recently, an isotopic neptunyl compound has been reported [34].

One of the most remarkable topological types within the uranyl selenite family of compounds is the phosphuranylite topology (Figure 3g,h): The crystal structures of marthozite, guilleminite, and larisaite are based on such layers, while haynesite and piritite (although their structures are still unknown) are supposed to have topologically the same architecture due to the similarity of their unit-cell parameters. Except for minerals, two more Li- and Sr-bearing synthetic uranyl selenites have structures based on the 2D units belonging to the phosphuranylite anion topology. The phosphuranylite topology contains two types of alternating infinite chains: Edge-sharing dimers of pentagons that are further linked by edge-sharing hexagons, and zig-zag chains of edge-sharing triangles and squares [80,83]. The topology can be described by the $6^15^24^23^2$ ring symbol with pentagons and hexagons occupied by Ur , triangles are occupied by selenite anions, while squares stay vacant. In the crystal structures of natural and synthetic compounds, additional mono-, divalent cations, and H_2O molecules are arranged in between the layers forming covalent and H-bonding systems to build the 3D structure. In the structure of marthozite, there are Cu^{2+} cations arranged in between the layers and octahedrally coordinated by two O atoms of uranyl ions from the above and underlying layers and four O atoms of H_2O molecules from the interlayer space. There are also four ‘zeolite’-like H_2O molecules arranged in the interlayer space, which are not covalently bonded to cations and held in the structure by H-bonds only. Na^+ and K^+ sites in the structure of larisaite are characterized by partial occupancies, as well as H_2O molecules and hydronium cations, which are statistically distributed over six sites within the interlayer space. Thus, there are also two types of H_2O molecules, those which coordinate alkali cations and ‘zeolite’-like, as in the structure of marthozite. Na^+ and K^+ cations in the crystal structure of larisaite

alternately occupy neighbor cavities in the interlayer space, while in the structure of guilleminite, those cavities are equivalent and occupied only by Ba^{2+} cations. It is of interest that according to previous works [1,27], only two sites of H_2O molecules coordinating Ba^{2+} cations have been determined in the structure of guilleminite, leaving rather a large cavity to be vacant. Our single crystal XRD studies at low temperatures allowed us to determine the third site arranged within the void and occupied by the H_2O molecule, which suggests a change to the formula of guilleminite to $\text{Ba}[(\text{UO}_2)_3(\text{SeO}_3)_2\text{O}_2](\text{H}_2\text{O})_4$. Such ambiguity allows reference to the variable character of H_2O molecules' amount within these structures, which could depend on the chemical composition and conditions, and the temperature and humidity storage of samples. Another interesting feature is that the structures of natural and synthetic compounds belong to different geometrical isomers. The (ud)(du) isomer was determined in the structures of Li- and Sr-bearing synthetic uranyl selenites, while (ud)(ud) isomer was observed in the crystal structures of all three minerals. It should be noted that implementation of the (ud)(du) isomer results in formation of stepped layers, in which each subsequent chain of edge-sharing uranyl polyhedra is located above the level of the previous chain, whereas the (ud)(ud) isomer results in the formation of zig-zag uranyl selenite layers, in which the chains of edge-sharing uranyl polyhedra are alternately located above or below the mean plane of the layer (Figure 4).

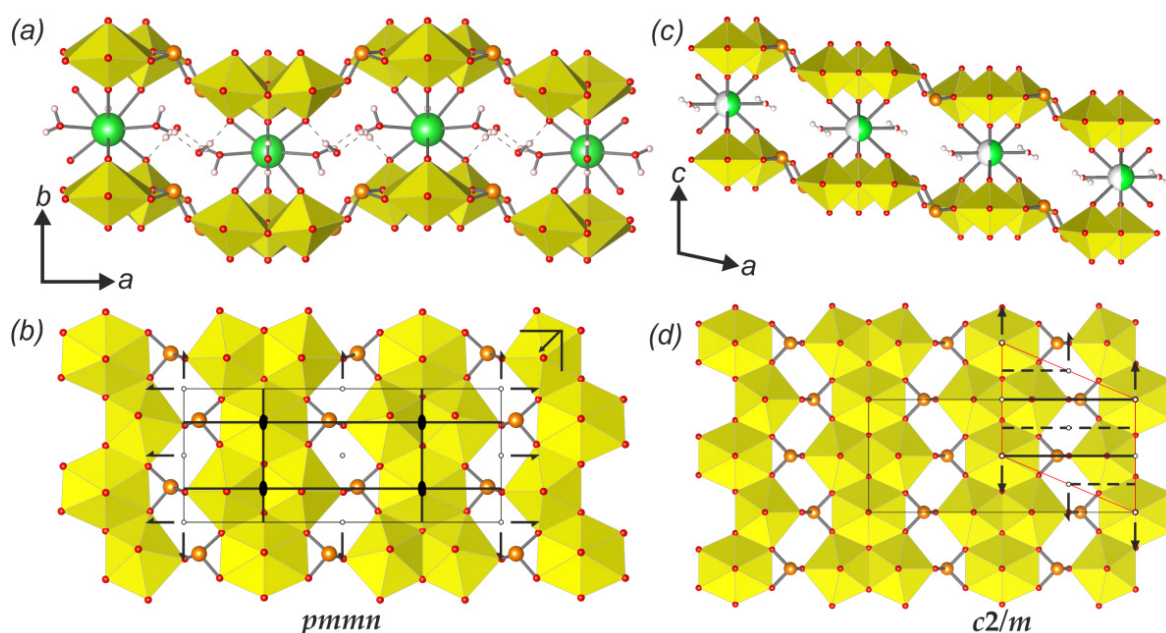


Figure 4. (a–d) The crystal structure projections along the layers, uranyl selenite layers, symmetry elements, and the respective layer symmetry groups for guilleminite (a,b) and $\text{Sr}[(\text{UO}_2)_3(\text{SeO}_3)_2\text{O}_2](\text{H}_2\text{O})_4$ (c,d). Legend: see Figure 1.

Another topology that consists of hexagons, pentagons, squares, and triangles can be described by the $6^15^34^63^5$ ring symbol (Figure 3i,j), and is quite rare. There are only three compounds known, whose structures are based on the layers of this type. Two of them are Cs-bearing [46] and organically templated [58] uranyl selenites, and the third one is a very exotic $\text{Cs}_2[(\text{UO}_2)_4(\text{Co}(\text{H}_2\text{O})_2)_2(\text{HPO}_4)(\text{PO}_4)]$ uranyl phosphate compound [84]. Layers are formed by the specific heptamers, and the uranyl hexagonal bipyramid is in the center, sharing each even equatorial edge with three uranyl pentagonal bipyramids, while the odd edges are shared with $[\text{SeO}_3]^{2-}$ groups. The linkage of these heptamers occurs via the third non-shared vertex of the selenite group and by the two additional selenite groups of each pentagonal bipyramid, which share all three O atoms with three neighbor heptamers. Thus, all pentagons and hexagons in the anion topology are occupied by the uranyl ions, triangles, and by the selenite groups while squares are vacant. It should be noted, that the arrangement of the lone electron pair in the structures of both uranyl selenites is different. In the structure of Cs-bearing uranyl

selenite, the orientation of the lone electron pairs around the core of uranyl bipyramids is uneven and can be described by the (uuudduuuudd) matrix, while that in the structure of organically templated uranyl selenite is uniform (uududuuddudd), but it does not result in any visible differences in the distortion or undulations between the layers.

The crystal structure of the Cs-bearing uranyl selenite-selenate **31** [46] phase is based on the layers of a highly remarkable anion topology with the $6^15^64^63^6$ ring symbol (Figure 3k,l), which could be assumed as the modular structure, composed of blocks from both the phosphuranylite and zippeite anion topologies. The latter, for instance, is one of the most common topologies among the natural uranyl sulfates [25]. The zippeite fragment of the topology includes selenate tetrahedra, and the phosphuranylite fragment contains selenite groups.

The crystal structure of the only uranyl diselenite compound [47] is based on the sheets of miscellaneous anion topology of the $8^15^23^8$ type (Figure 3m,n), consisting of octagons, pentagons, and triangles. The layered complex is built by the dimers of edge-sharing uranyl pentagonal bipyramids, which are arranged similarly as in the structures of such minerals as deliensite, $\text{Fe}[(\text{UO}_2)_2(\text{SO}_4)_2(\text{OH})_2](\text{H}_2\text{O})_7$ [85] or plášilite, $\text{Na}(\text{UO}_2)(\text{SO}_4)(\text{OH})(\text{H}_2\text{O})_2$ [86], but the linkage character is remarkably different. Instead of isolated groups, uranyl dimers are interlinked length- and side-ways through the vertex-sharing diselenite groups; besides, lone electron pairs within the $[\text{Se}_2\text{O}_5]^{2-}$ oxyanions are co-directed. In those diselenite groups, which are arranged along the extension of the uranyl dimers, lone electron pairs are oriented towards one side relative to the plane of the sheet, and in those groups, arranged side-ways, the direction of the lone electron pair is the opposite. The crystal structure of **32** is anhydrous and free of additional ions, thus electroneutral layered complexes are linked into the 3D structure by the means of electrostatic interactions involving lone electron pairs only.

3.4. Structural and Topological Complexity

Calculation was performed in several stages and the main results are summarized in Table 3 and Figures 5 and 6. First, the topological complexity (TI), according to the maximal rod (for chains) or layer symmetry group, was calculated, since these are the basic structural units. Second, the structural complexity (SI) of the units was analyzed taking into account its real symmetry. The next contribution to information comes from the stacking (LS) of chained and layered complexes (if more than one layer or chain is in the unit cell). The fourth contribution to the total structural complexity is given by the interstitial structure (IS). The last portion of information comes from the interstitial H bonding system (H). It should be noted that the H atoms related to the U-bearing chains and layers were considered as a part of those complexes but not within the contribution of the H-bonding system. Complexity parameters for the whole structures were calculated using *ToposPro* package [87].

Table 3. Structural and topological complexity parameters for the uranyl selenite and selenite-selenate compounds.

No.	Formula	Topology	Complexity Parameters of the Crystal Structure				Structural Complexity of the U-Se Unit				Topological Complexity of the U-Se Unit			
			Sp. Gr.	ν	I_G	$I_{G,total}$	Layer or Rod Sym. Gr.	ν	I_G	$I_{G,total}$	Layer or Rod Sym. Gr.	ν	I_G	$I_{G,total}$
Chains														
1	$\text{Cu}_4[(\text{UO}_2)(\text{SeO}_3)_2](\text{OH})_6/\text{derriksite}$	cc1-1:2-1	$Pn2_1m$	54	4.236	228.764	t_cm11	11	3.096	34.054	$t_a2/m11$	11	2.187	24.054
8	$[(\text{UO}_2)(\text{HSeO}_3)_2(\text{H}_2\text{O})]$		$A2/a$	32	3.125	100.000	$t_a12/a1$	32	3.125	100.000	$t_a12/a1$	32	3.125	100.000
9	$[(\text{UO}_2)(\text{HSeO}_3)_2](\text{H}_2\text{O})$		$C2/c$											
2	$\text{Pb}_2\text{Cu}_5[(\text{UO}_2)_2(\text{SeO}_3)_6(\text{OH})_6](\text{H}_2\text{O})_2/\text{demesmaeckerite}$	cc1-1:3-2	$P-1$	55	4.800	263.975	$t-1$	30	3.907	117.207	$t_a2_1/m11$	30	3.374	101.207
33	$[\text{C}_4\text{H}_{12}\text{N}][(\text{UO}_2)(\text{SeO}_3)(\text{NO}_3)]$	cc1-1:2-12	$C2/m$	56	4.236	237.212	$t_a2_1/m11$	22	3.096	68.108	$t_a2_1/m11$	22	3.096	68.108
10	$\text{Ca}[(\text{UO}_2)(\text{SeO}_3)_2]$	cc1-1:2-14	$P-1$	24	3.585	86.039	$t-1$	22	3.459	76.108	$t-1$	22	3.459	76.108
11	$\text{Sr}[(\text{UO}_2)(\text{SeO}_3)_2]$													
12	$\text{Sr}[(\text{UO}_2)(\text{SeO}_3)_2](\text{H}_2\text{O})_2$	cc1-1:2-15	$P-1$	36	4.170	150.117	$t-1$	22	3.459	76.108	$t-1$	22	3.459	76.108
13	$\text{Na}_3[\text{H}_3\text{O}][(\text{UO}_2)(\text{SeO}_3)_2]_2(\text{H}_2\text{O})$			64	5.000	320.000								
Layers with corner-linkage														
14	$[\text{NH}_4]_2[(\text{UO}_2)(\text{SeO}_3)_2](\text{H}_2\text{O})_{0.5}$	cc2-1:2-4	$P2_1/c$	94	4.576	430.131	$p2_1/b$	44	3.459	152.196	$p2_1/b$	44	3.459	152.196
15	$[\text{NH}_4][(\text{UO}_2)(\text{SeO}_3)(\text{HSeO}_3)]$		$P2_1/n$	68	4.087	277.947	$p2_1/b$	48	3.585	172.080		48	3.585	172.080
16	$\text{K}[(\text{UO}_2)(\text{HSeO}_3)(\text{SeO}_3)]$		$P2_1/n$	52	3.700	192.423	$p2_1/b$	48	3.585	172.080				
17	$\text{Rb}[(\text{UO}_2)(\text{HSeO}_3)(\text{SeO}_3)]$		$P2_1/n$	52	3.700	192.423	$p2_1/b$	48	3.585	172.080				
18	$\text{Cs}[(\text{UO}_2)(\text{HSeO}_3)(\text{SeO}_3)]$		$P2_1/c$	104	4.700	488.846	$p2_1$	48	4.585	172.080				
19	$\text{Cs}[((\text{U,Np})\text{O}_2)(\text{HSeO}_3)(\text{SeO}_3)]$		$P2_1/n$	52	3.700	192.423	$p2_1/b$	48	3.585	172.080				
20	$\text{Ti}[(\text{UO}_2)(\text{HSeO}_3)(\text{SeO}_3)]$		$P2_1/n$	52	3.700	192.423	$p2_1/b$	48	3.585	172.080				
21	$\text{Cs}[(\text{UO}_2)(\text{SeO}_3)(\text{HSeO}_3)](\text{H}_2\text{O})_3$		$P2_1/n$	88	4.459	392.430	$p2_1/b$	48	3.585	172.080				
22	$\text{Na}[(\text{UO}_2)(\text{SeO}_3)(\text{HSeO}_3)](\text{H}_2\text{O})_4$		$P2_1/n$	100	4.644	464.386	$p2_1/b$	48	3.585	172.080				
34	$[\text{C}_6\text{H}_{14}\text{N}_2]_{0.5}[(\text{UO}_2)(\text{HSeO}_3)(\text{SeO}_3)](\text{H}_2\text{O})_{0.5}(\text{CH}_3\text{CO}_2\text{H})_{0.5}$		$Pnma$	228	4.991	1137.899	$p2_1/b$	48	3.585	172.080				
35	$[\text{C}_4\text{H}_{12}\text{N}_2]_{0.5}[(\text{UO}_2)(\text{HSeO}_3)(\text{SeO}_3)]$		$P2_1/c$	84	4.392	368.955	$p2_1/b$	48	3.585	172.080				
36	$[(\text{C}_2\text{H}_8\text{N}_2)\text{H}_2][(\text{UO}_2)(\text{SeO}_3)(\text{HSeO}_3)](\text{NO}_3)(\text{H}_2\text{O})_{0.5}$		$Pbca$	264	5.044	1331.720	$p2_1/b$	48	3.585	172.080				

Table 3. Cont.

No.	Formula	Topology	Complexity Parameters of the Crystal Structure				Structural Complexity of the U-Se Unit				Topological Complexity of the U-Se Unit			
			Sp. Gr.	ν	I_G	$I_{G,total}$	Layer or Rod Sym. Gr.	ν	I_G	$I_{G,total}$	Layer or Rod Sym. Gr.	ν	I_G	$I_{G,total}$
23	[H ₃ O][(UO ₂)(SeO ₄)(HSeO ₃)]		$P2_1/n$	68	4.087	277.947								
37	[C ₅ H ₁₄ N][(UO ₂)(SeO ₄)(HSeO ₃)]		$P2_1/n$	132	5.044	665.860	$p2_1/b$	52	3.700	192.423		52	3.700	192.423
38	[C ₂ H ₈ N][(UO ₂)(SeO ₄)(HSeO ₃)]		$P2_1/n$	96	4.585	440.156								
39	[C ₅ H ₆ N][(UO ₂)(SeO ₄)(HSeO ₃)]		$P2_1/n$	100	4.644	464.386								
40	[C ₉ H ₂₄ N ₂][(UO ₂)(SeO ₄)(HSeO ₃)](NO ₃)		$P-1$	208	6.700	1393.691								
24	Ag ₂ [(UO ₂)(SeO ₃) ₂]	cc2-1:2-5	$P2_1/n$	52	3.700	192.423	$p2_1/b$	44	3.459	152.215	$p2_1/b$	44	3.459	152.215
41	[C ₂ H ₈ N][(H ₅ O ₂)(H ₂ O)] [(UO ₂) ₂ (SeO ₄) ₃ (H ₂ SeO ₃)](H ₂ O)	cc2-1:2-14	$P2_1/n$	204	5.672	1157.175	$p2_1/b$	104	4.755	513.528	$p2_1/b$	104	4.755	513.528
42	[C ₄ H ₁₅ N ₃][H ₃ O] _{0.5} [(UO ₂) ₂ (SeO ₄) _{2.93} (SeO ₃) _{0.07} (H ₂ O)](NO ₃) _{0.5}	cc2-2:3-4	$P2_1/c$	212	5.728	1214.319	$p2_1$	48	4.585	220.078	$p2_1$	48	4.585	220.078
43	[C ₅ H ₁₄ N] ₄ [(UO ₂) ₃ (SeO ₄) ₄ (HSeO ₃)(H ₂ O)](H ₂ SeO ₃)(HSeO ₄)	cc2-3:5-3	$P-1$	258	7.011	1808.897	$p-1$	74	5.209	385.500	$p2_1/m$	74	4.399	325.500
44	[C ₂ H ₈ N] ₃ (C ₂ H ₇ N) [(UO ₂) ₃ (SeO ₄) ₄ (HSeO ₃)(H ₂ O)]		$Pnma$	364	5.629	2048.837	$p2_1/m$	74	4.399	325.500				
45	[C ₂ H ₈ N] ₂ [H ₃ O][(UO ₂) ₃ (SeO ₄) ₄ (HSeO ₃)(H ₂ O)](H ₂ SeO ₃) _{0.2}		$P2_1/m$	134	5.200	696.856								
Layers with Edge-Linkage														
25	Pb[(UO ₂)(SeO ₃) ₂]	cc2-1:2-19	$Pmc2_1$	48	3.835	184.078	$p2_1ma$	44	3.641	160.215	$p2_1ma$	44	3.641	160.215
26	Ba[(UO ₂)(SeO ₃) ₂]	cc2-1:2-21	$P2_1/c$	48	3.585	172.078	$p2_1/a$	44	3.459	152.215	$p2_1/a$	44	3.459	152.215
27	[(UO ₂)(SeO ₃)]	6 ¹ 3 ²	$P2_1/m$	14	2.236	31.303	$p2_1/m$	14	2.236	31.303	$p2_1/m$	14	2.236	31.303
3	Cu[(UO ₂) ₃ (SeO ₃) ₂ O ₂] (H ₂ O) ₈ / marthozite	6 ¹ 5 ² 4 ² 3 ²	$Pbn2_1$	176	5.459	960.860	pn	38	4.248	161.421	$pmmn$	38	3.195	121.421
4	Ba[(UO ₂) ₃ (SeO ₃) ₂ O ₂] (H ₂ O) ₄ / guilleminite		$Pmn2_1$	70	4.386	307.050	$p2_1mn$	38	3.511	133.421				
5	Na(H ₃ O)[(UO ₂) ₃ (SeO ₃) ₂ O ₂] (H ₂ O) ₄ / larisaite		$P11m$	73	5.395	393.857	pm	38	4.511	171.421				
28	Sr[(UO ₂) ₃ (SeO ₃) ₂ O ₂](H ₂ O) ₄		$C2/m$	28	3.450	96.606	$c2/m$	19	3.090	58.711				
29	Li ₂ [(UO ₂) ₃ (SeO ₃) ₂ O ₂](H ₂ O) ₆		$P2_1/c$	78	4.311	336.261	$p2_1/a$	38	3.301	125.421				

Table 3. Cont.

No.	Formula	Topology	Complexity Parameters of the Crystal Structure				Structural Complexity of the U-Se Unit				Topological Complexity of the U-Se Unit			
			Sp. Gr.	ν	I_G	$I_{G,total}$	Layer or Rod Sym. Gr.	ν	I_G	$I_{G,total}$	Layer or Rod Sym. Gr.	ν	I_G	$I_{G,total}$
30	Cs ₂ [(UO ₂) ₄ (SeO ₃) ₅](H ₂ O) ₂	6 ¹ 5 ³ 4 ⁶ 3 ⁵	<i>P</i> 2 ₁ / <i>n</i>	160	5.322	851.508	<i>pn</i>	64	5.000	320.000	<i>p</i> 2 ₁ <i>mn</i>	64	4.250	272.000
46	[C ₈ H ₁₅ N ₂] ₂ [(UO ₂) ₄ (SeO ₃) ₅]		<i>Pnma</i>	328	5.455	1789.277	<i>p</i> 2 ₁ <i>mn</i>	64	4.250	272.000		64	4.250	272.000
31	Cs ₂ [(UO ₂) ₇ (SeO ₄) ₂ (SeO ₃) ₂ (OH) ₄ O ₂](H ₂ O) ₅	6 ¹ 5 ⁶ 4 ⁶ 3 ⁶	<i>P</i> 2 ₁ / <i>m</i>	132	5.226	689.860	<i>p</i> -1	49	4.635	227.121	<i>p</i> -1	49	4.635	227.121
32	UO ₂ Se ₂ O ₅	8 ¹ 5 ² 3 ⁸	<i>P</i> -1	40	4.322	172.877	<i>p</i> 1	20	4.322	86.439	<i>p</i> 2	20	3.422	68.439

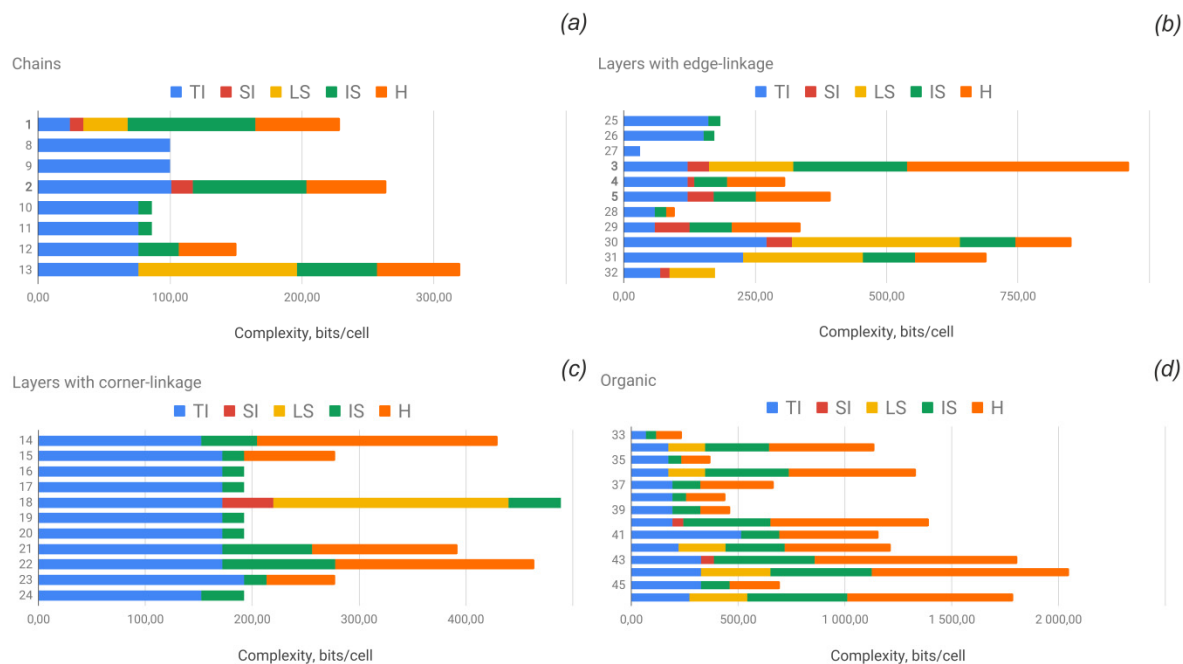


Figure 5. Ladder diagrams showing contributions of various factors to structural complexity in terms of bits per unit cell for the structures based on chains (a), layers with edge-linkage of polyhedra (b), layers with corner-linkage of polyhedra (c) and organically templated compounds (d). Legend: TI = topological information; CI = cluster information (valid for Prw and Nsb: See text for details); SI = structural information; LS = layer stacking; IS = interstitial structure; HB = hydrogen bonding. See Table 3 and text for details.

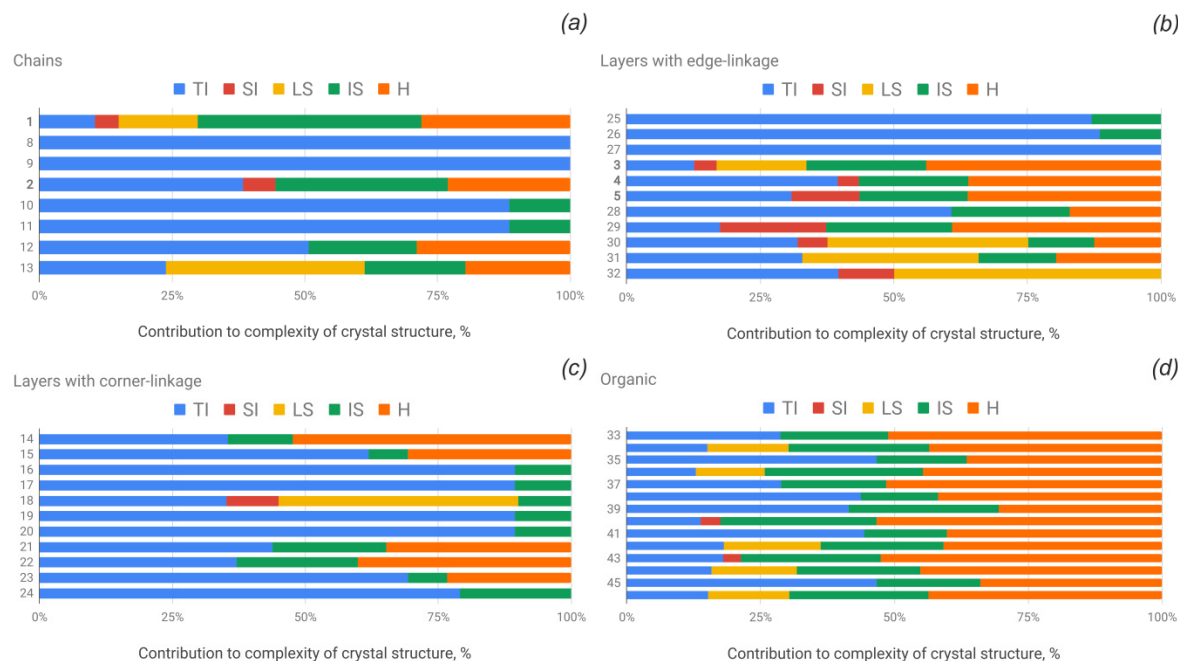


Figure 6. Ladder diagrams showing normalized contributions (in %) of various factors to structural complexity for the structures based on chains (a), layers with edge-linkage of polyhedra (b), layers with corner-linkage of polyhedra (c) and organically templated compounds (d). Legend: see Figure 5. See Table 3 and text for details.

4. Discussion

Structural features of natural uranyl selenites make one think about the conditions of their formation in nature. Analogies with synthetic compounds, which have a similar structure, allow some of the most probable pathways to be suggested. The formation of structural units with edge-sharing polyhedra in most cases indicates their hydrothermal origin, and the synthetic uranyl selenites **28** and **29**, whose structures are built upon the layers with a phosphuranylite topology (Figure 3g), are no exception. Both compounds were obtained from the aqueous medium at temperatures above 220 °C. In the case of compounds with structures based upon 1D units, the situation is somewhat more complicated. Topological type $cc1-1:2-1$, which is one of the most common among the U(VI)-bearing oxysalts, was repeatedly observed in the structures of compounds obtained at room temperature. However, synthetic uranyl selenite **9** was grown at slightly higher temperatures of 80 °C. Moreover, the presence of rather specific uranyl tetragonal bipyramids in the structure of derriksite refers to a family of isotypic uranyl phosphate [88], molybdate [89], and tellurite [90] compounds, which were obtained during hydrothermal (above 180 °C) or high temperature solid state (above 650 °C) syntheses. Analogously, the crystal structures of synthetic uranyl chromates [67,68] and molybdates [69], which are isotypic to that one of demesmaekerite, were obtained at hydrothermal conditions (above 120 °C) or solid state reactions (at 300 °C). Nevertheless, based on laboratory [91,92] and field observations, namely of the mineral association from Zálesí (Czech Republic) [8], it is clear that demesmaekerite and piretite (and several other unnamed or poorly identified U-Se phases) formed as a result of supergene alteration processes, which exclude hydrothermal activity. These observations are supported by the radioanalytical dating of demesmaekerite.

The crystal structure of derriksite is built on the 1D uranyl selenite complexes, whose symmetry is described by the $t_c m 11$ rod symmetry group. However, its highest (topological) symmetry is described by the centrosymmetric $t_a 2/m 11$ rod group (Figure 7a). Stacking of chains doubles the complexity contribution of the uranyl selenite block (68.107 bits/cell) into the whole structure, but is still less than the contribution of the Cu-O interstitial block (96.370 bits/cell) and nearly equal to the contribution of the interstitial H-bonding system (64.287 bits/cell; Figure 5 and 6). Alteration of uranyl tetragonal bipyramids by pentagonal ones with the additional H₂O molecule in the equatorial plane of *Ur* preserves the topology, but it doubles the size of the reduced segment of a chain and changes its maximal symmetry to the $t_a 2/m 11$ rod group (Figure 7b). The absence of the interstitial substructure makes the topological complexity parameters be equal to those for the whole structure of **8** and **9**.

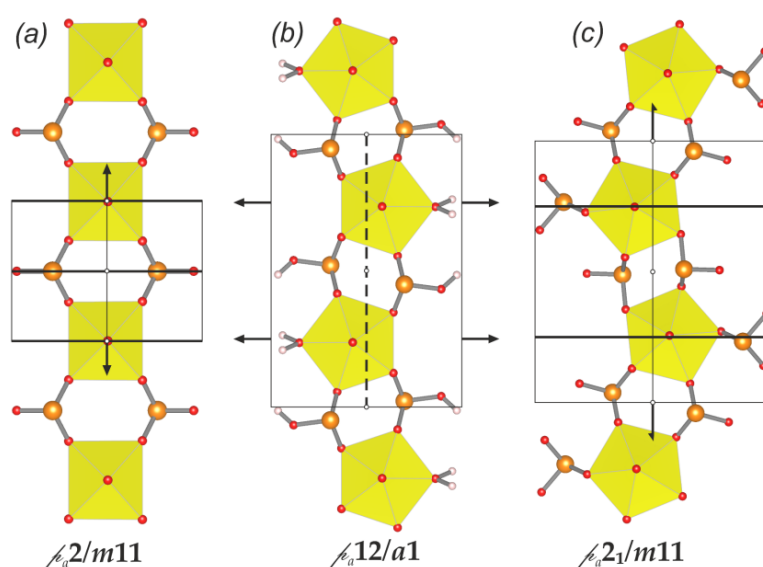


Figure 7. 1D uranyl selenite units and their highest rod symmetry groups for derriksite (a), [(UO₂)(HSeO₃)₂(H₂O)] (b) and demesmaekerite (c). Legend: see Figure 1.

The topological symmetry of the uranyl selenite chain in the structure of demesmaekerite is monoclinic $b_a2_1/m11$ and is higher than its real triclinic $b-1$ symmetry (Figure 7c). In this case, the uranyl selenite substructure (117.207 bits/cell) makes the largest contribution to the complexity of the whole structure. The interstitial complex contributes a slightly lower amount of information (85.926 bits/cell), and even less is accounted for in the H-bonding system (60.842 bits/cell; Figure 5 and 6).

The crystal structures of 17 uranyl selenites and selenite-selenates are built upon the layers of $cc1-1:2-4$ topological type and those are distributed almost equally between pure inorganic and organically templated compounds having various monovalent inorganic ions and protonated amine molecules of different shapes and sizes as an interstitial block. Moreover, this topology preserves changes in the chemical composition of uranyl-bearing layers, which involves the occurrence of uranyl selenites, selenite-hydrogen selenites, and hydrogen selenite-selenates. It is of interest that all isomers within this family of compounds, including chemical substitutions and two geometrical isomers (see Chapter 3.3.), have the highest symmetry of the layer described by the $p2_1/b$ layer group (Figure 8). Furthermore, the topological symmetry is preserved in the structures of almost all compounds, except for two of them (Table 3). All three aforementioned cases point to the fact that the current topological type is unusually resistant and one of the most preferable in the systems with the U:T ratio = 1:2. As for the complexity calculations, certainly, those will primarily depend on the number of orbits (atoms). Thus, the H-free uranyl selenite layer has the lowest amount of information (152.196 bits/cell), next in a row would be the uranyl selenite-hydrogen selenite complex (172.080 bits/cell), and finally those containing selenate oxyanions (192.423 bits/cell). Analogously, complexity parameters for the whole structure majorly depend on the size of the aliphatic part of organic molecules.

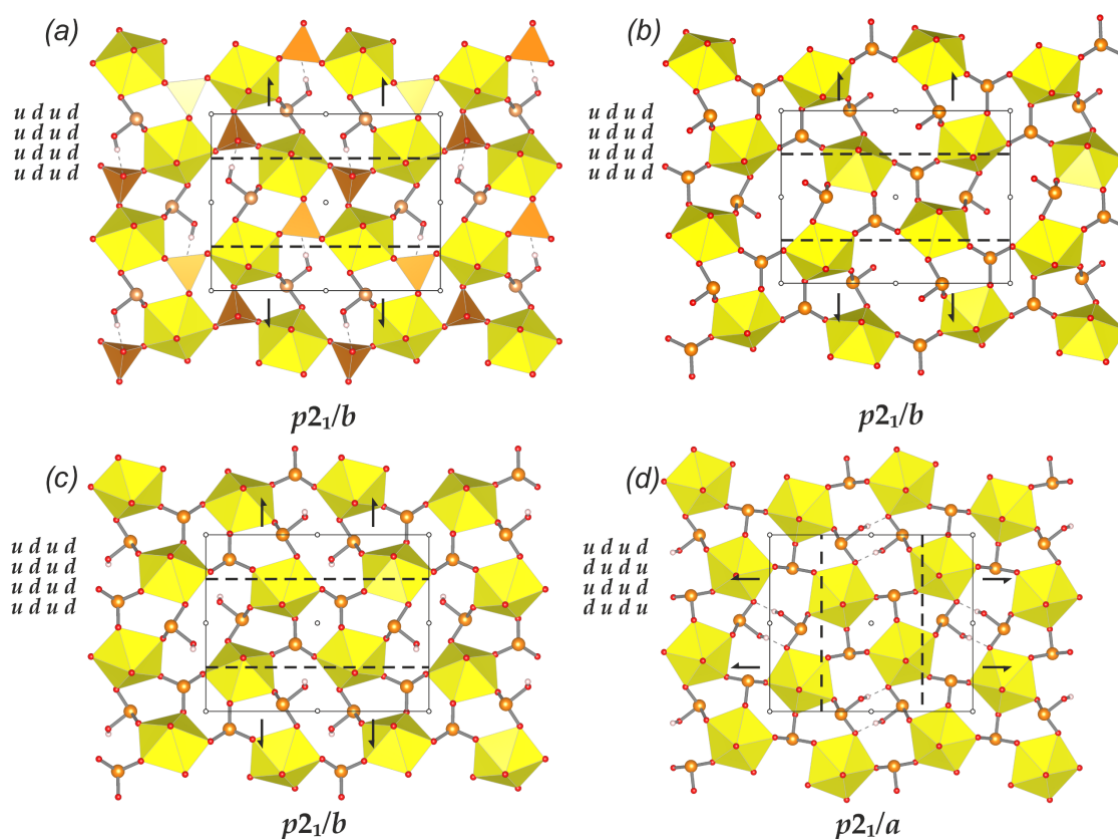


Figure 8. (a–d) Uranyl selenite layers, symmetry elements, and the respective layer symmetry groups for various isomers of the $cc1-1:2-4$ topological type (a–d: see text for details). Legend: see Figures 1 and 2.

The crystal structures of three uranyl selenite minerals and two synthetic compounds are based on dense layers with a phosphuranylite anion topology. It is of interest that natural and synthetic compounds are described by the different orientation matrices (Figure 4). The (ud)(du) orientation of the lone electron pairs in the structures of synthetic uranyl selenites **28** and **29** resulted in the formation of layers with the $c2/m$ topological symmetry (58.711 bits/cell), whereas the highest symmetry of those in natural compounds is described by the (ud)(ud) matrix and orthorhombic $pmmn$ layer symmetry group (121.421 bits/cell). It should be noted that only Sr-bearing synthetic compound **28** has the real symmetry of the layer equal to the topological one. In the cases of marthozite, guileminite, larisaite, and Li-bearing synthetic compound, topological symmetry is significantly reduced by the interstitial cations and H₂O molecules (Table 3, Figures 4 and 5). The contribution of each of the components makes the marthozite the most complex inorganic uranyl selenite (960.860 bits/cell; Figures 5 and 6). It is of interest that the formation of a particular isomer causes the specific arrangement of the layers, and it appears that the (ud)(ud) isomer of the phosphuranylite topology, which results in the formation of zig-zag layers, is more stable and most likely thermodynamically preferable among the others, since it has only been observed in the structures of natural layered uranyl selenites.

5. Conclusions

The refinement of the demesmaekerite crystal structure makes it possible to determine the H atoms positions belonging to the interstitial H₂O molecules. The refinement of the guileminite crystal structure allows the determination of one additional site arranged within the void of the interlayer space and occupied by the H₂O molecule, which suggests the formula of guileminite to be written as Ba[(UO₂)₃(SeO₃)₂O₂](H₂O)₄ instead of Ba[(UO₂)₃(SeO₃)₂O₂](H₂O)₃.

Our numerous attempts to determine the crystal structure of haynesite, [(UO₂)₃(SeO₃)₂(OH)₂](H₂O)₅, were unsuccessful. However, several assumptions could be made. First, the presence of (OH)[−] groups within such a dense layer is doubtful. At least, there is no other evidence for O atoms' protonation in the structures of all the other natural and synthetic uranyl selenites, whose structures are built upon layers of the same topology. Moreover, the structure of haynesite has to be electroneutral, and H₂O molecules from the interlayer space should be replaced by H₃O⁺ cations, which points to the similarity and, probably, to the common genesis or even the closest relationships between the haynesite and larisaite, Na(H₃O)[(UO₂)₃(SeO₃)₂O₂](H₂O)₄.

Comparison of the isotopic natural and synthetic uranyl-bearing compounds suggests that uranyl selenite mineral formation requires heating, which most likely, keeping in mind their surface or near-surface occurrence conditions, can be attributed to the radioactive decay.

Structural complexity studies revealed an interesting tendency in that the majority of synthetic compounds have the topological symmetry of uranyl selenite building blocks equal to the structural symmetry, which means that the highest symmetry of uranyl complexes is preserved regardless of the interstitial filling of the structures. Whereas the real symmetry of chained and layered complexes in the structures of uranyl selenite minerals is lower than their topological symmetry, which means that interstitial cations and H₂O molecules significantly affect the structural architecture of natural compounds. At the same time, structural complexity parameters for the whole structure are usually higher for the minerals than that for synthetic compounds of a similar or close organization, which probably indicates the preferred existence of such natural-born architectures.

Supplementary Materials: The following are available online at <http://www.mdpi.com/2073-4352/9/12/639/s1>: Cif files for guileminite and demesmaekerite.

Author Contributions: Conceptualization, V.V.G. and J.P.; Methodology, V.V.G., V.M.K. and I.V.K.; Investigation, V.V.G., I.V.K., V.M.K., M.N.M., A.V.K. and J.P.; Writing-Original Draft Preparation, V.V.G., I.V.K., V.M.K., M.N.M., A.V.K. and J.P.; Writing-Review & Editing, V.V.G. and J.P.; Visualization, V.V.G. and I.V.K.

Funding: This research was funded by the Russian Science Foundation (grant 18-17-00018 to V.V.G. and I.V.K.) and through the project of the Ministry of Education, Youth and Sports National sustainability program I of the Czech Republic (project No. LO1603 to J.P.).

Acknowledgments: The XRD measurements of guilleminite have been performed at the X-ray Diffraction Centre of the St. Petersburg State University. We are grateful to reviewers for useful comments.

Conflicts of Interest: The authors declare no conflict of interest.

References

- Pierrot, R.; Toussaint, J.; Verbeek, T. La guilleminite, une nouvelle espèce minérale. *B. Soc. Fr. Minéral. Cr.* **1965**, *88*, 132–135. [\[CrossRef\]](#)
- Cesbron, F.; Bachet, B.; Oosterbosch, R. La demesmaekerite, sélénite hydraté d'uranium, cuivre et plomb. *Bulletin B. Soc. Fr. Minéral. Cr.* **1965**, *88*, 422–425. [\[CrossRef\]](#)
- Cesbron, F.; Oosterbosch, R.; Pierrot, R. Une nouvelle espèce minérale: La marthozite. Uranyl-sélénite de cuivre hydraté. *B. Soc. Fr. Minéral. Cr.* **1969**, *92*, 278–283. [\[CrossRef\]](#)
- Cesbron, F.; Pierrot, R.; Verbeek, T. La derriksite, $\text{Cu}_4(\text{UO}_2)(\text{SeO}_3)_2(\text{OH})_6 \cdot \text{H}_2\text{O}$, une nouvelle espèce minérale. *B. Soc. Fr. Minéral. Cr.* **1971**, *94*, 534–537.
- Deliens, M.; Piret, P. La haynesite, sélénite hydraté d'uranyle, nouvelle espèce minérale de la Mine Repete, Comté de San Juan, Utah. *Can. Mineral.* **1991**, *29*, 561–564.
- Vochten, R.; Bleton, N.; Peeters, O.; Deliens, M. Piretite, $\text{Ca}(\text{UO}_2)_3(\text{SeO}_3)_2(\text{OH})_4 \cdot 4\text{H}_2\text{O}$, a new calcium uranyl selenite from Shinkolobwe, Shaba, Zaire. *Can. Mineral.* **1996**, *34*, 1317–1322.
- Chukanov, N.V.; Pushcharovsky, D.Y.; Pasero, M.; Merlino, S.; Barinova, A.V.; Möckel, S.; Pekov, I.V.; Zadov, A.E.; Dubinchuk, V.T. Larisaite, $\text{Na}(\text{H}_3\text{O})(\text{UO}_2)_3(\text{SeO}_3)_2\text{O}_2 \cdot 4\text{H}_2\text{O}$, a new uranyl selenite mineral from Repete mine, San Juan County, Utah, U.S.A. *Eur. J. Mineral.* **2004**, *16*, 367–374. [\[CrossRef\]](#)
- Sejkora, J.; Škoda, R.; Pauliš, P. Selenium mineralization of the uranium deposit Zálesí, Rychlebské Hory Mts., Czech Republic. *Mineral. Pol.* **2006**, *28*, 196–198.
- Gelfort, E. Nutzung der spaltprodikhte nach aufarbeitung ausgedienter brennelemente. *Atomwirtsch. Atomtech.* **1985**, *30*, 32–36.
- Chen, F.; Burns, P.C.; Ewing, R.C. ^{79}Se : Geochemical and crystallo-chemical retardation mechanisms. *J. Nucl. Mater.* **1999**, *275*, 81–88. [\[CrossRef\]](#)
- CrysAlisPro Software System*; Version 1.171.38.46; Rigaku Oxford Diffraction: Oxford, UK, 2015.
- Sheldrick, G.M. SHELXT—Integrated space-group and crystal structure determination. *Acta Crystallogr.* **2015**, *A71*, 3–8. [\[CrossRef\]](#) [\[PubMed\]](#)
- Sheldrick, G.M. Crystal structure refinement with SHELXL. *Acta Crystallogr.* **2015**, *C71*, 3–8.
- Dolomanov, O.V.; Bourhis, L.J.; Gildea, R.J.; Howard, J.A.K.; Puschmann, H. OLEX2: A complete structure solution, refinement and analysis program. *J. Appl. Cryst.* **2009**, *42*, 339–341. [\[CrossRef\]](#)
- Petríček, V.; Dušek, M.; Palatinus, L. Crystallographic computing system JANA2006: General features. *Z. Kristallogr.* **2014**, *229*, 345–352. [\[CrossRef\]](#)
- Krivovichev, S.V. Combinatorial topology of salts of inorganic oxoacids: Zero-, one- and two-dimensional units with corner-sharing between coordination polyhedra. *Crystallogr. Rev.* **2004**, *10*, 185–232. [\[CrossRef\]](#)
- Burns, P.C.; Miller, M.L.; Ewing, R.C. U^{6+} minerals and inorganic phases: A comparison and hierarchy of structures. *Can. Mineral.* **1996**, *34*, 845–880.
- Krivovichev, S.V. *Structural Crystallography of Inorganic Oxysalts*; Oxford University Press: Oxford, UK, 2008; 303p.
- Krivovichev, S.V. Topological complexity of crystal structures: Quantitative approach. *Acta Crystallogr.* **2012**, *A68*, 393–398. [\[CrossRef\]](#)
- Krivovichev, S.V. Structural complexity of minerals: Information storage and processing in the mineral world. *Mineral. Mag.* **2013**, *77*, 275–326. [\[CrossRef\]](#)
- Krivovichev, S.V. Which inorganic structures are the most complex? *Angew. Chem. Int. Ed.* **2014**, *53*, 654–661. [\[CrossRef\]](#)
- Krivovichev, S.V. Structural complexity of minerals and mineral parageneses: Information and its evolution in the mineral world. In *Highlights in Mineralogical Crystallography*; Danisi, R., Armbruster, T., Eds.; Walter de Gruyter GmbH: Berlin, Germany; Boston, MA, USA, 2015; pp. 31–73.
- Krivovichev, S.V. Structural complexity and configurational entropy of crystalline solids. *Acta Crystallogr.* **2016**, *B72*, 274–276.
- Krivovichev, S.V. Ladders of information: What contributes to the structural complexity in inorganic crystals. *Z. Kristallogr.* **2018**, *233*, 155–161. [\[CrossRef\]](#)

25. Gurzhiy, V.V.; Plasil, J. Structural complexity of natural uranyl sulfates. *Acta Crystallogr.* **2019**, *B75*, 39–48. [[CrossRef](#)]
26. Krivovichev, V.G.; Krivovichev, S.V.; Charykova, M.V. Selenium minerals: Structural and chemical diversity and complexity. *Minerals* **2019**, *9*, 455. [[CrossRef](#)]
27. Cooper, M.A.; Hawthorne, F.C. The crystal structure of guilleminite, a hydrated Ba–U–Se sheet structure. *Can. Mineral.* **1995**, *33*, 1103–1109.
28. Ginderow, D.; Cesbron, F. Structure de la demesmaekerite, $\text{Pb}_2\text{Cu}_5(\text{SeO}_3)_6(\text{UO}_2)_2(\text{OH})_6 \cdot 2\text{H}_2\text{O}$. *Acta Crystallogr.* **1983**, *C39*, 824–827.
29. Cooper, M.A.; Hawthorne, F.C. Structure topology and hydrogen bonding in marthozite, $\text{Cu}^{2+}[(\text{UO}_2)_3(\text{SeO}_3)_2\text{O}_2](\text{H}_2\text{O})_8$, a comparison with guilleminite, $\text{Ba}[(\text{UO}_2)_3(\text{SeO}_3)_2\text{O}_2](\text{H}_2\text{O})_3$. *Can. Mineral.* **2001**, *39*, 797–807. [[CrossRef](#)]
30. Ginderow, D.; Cesbron, F. Structure de la derriksite, $\text{Cu}_4(\text{UO}_2)(\text{SeO}_3)_2(\text{OH})_6$. *Acta Crystallogr.* **1983**, *C39*, 1605–1607.
31. Cejka, J.; Sejkora, J.; Deliens, M. To the infrared spectrum of haynesite, a hydrated uranyl selenite, and its comparison with other uranyl selenites. *Neues Jahrbuch Mineral. Monatshefte* **1999**, *6*, 241–252.
32. Frost, R.L.; Weier, M.L.; Reddy, B.J.; Cejka, J. A Raman spectroscopic study of the uranyl selenite mineral haynesite. *J. Raman Spectrosc.* **2006**, *37*, 816–821. [[CrossRef](#)]
33. Loopstra, B.O.; Brandenburg, N.P. Uranyl selenite and uranyl tellurite. *Acta Crystallogr.* **1978**, *B34*, 1335–1337. [[CrossRef](#)]
34. Diefenbach, K.; Lin, J.; Cross, J.N.; Dalal, N.S.; Shatruk, M.; Albrecht-Schmitt, T.E. Expansion of the rich structures and magnetic properties of neptunium selenites: Soft ferromagnetism in $\text{Np}(\text{SeO}_3)_2$. *Inorg. Chem.* **2014**, *53*, 7154–7159. [[CrossRef](#)]
35. Mistryukov, V.E.; Mikhailov, Y.N. Structural features of the selenite group in uranyl complexes with neutral ligands. *Koordinats. Khim.* **1983**, *9*, 97–102.
36. Koskenlinna, M.; Mutikainen, I.; Leskela, T.; Leskela, M. Low-temperature crystal structures and thermal decomposition of uranyl hydrogen selenite monohydrate, $[(\text{UO}_2)(\text{HSeO}_3)_2](\text{H}_2\text{O})$ and diammonium uranyl selenite hemihydrate, $[\text{NH}_4]_2[(\text{UO}_2)(\text{SeO}_3)_2](\text{H}_2\text{O})_{0.5}$. *Acta Chem. Scand.* **1997**, *51*, 264–269. [[CrossRef](#)]
37. Almond, P.M.; Peper, S.; Bakker, E.; Albrecht-Schmitt, T.E. Variable dimensionality and new uranium oxide topologies in the alkaline-earth metal uranyl selenites $\text{AE}[(\text{UO}_2)(\text{SeO}_3)_2]$ ($\text{AE} = \text{Ca}, \text{Ba}$) and $\text{Sr}[(\text{UO}_2)(\text{SeO}_3)_2] \cdot 2\text{H}_2\text{O}$. *J. Solid State Chem.* **2002**, *168*, 358–366. [[CrossRef](#)]
38. Almond, P.M.; Albrecht-Schmitt, T.E. Hydrothermal synthesis and crystal chemistry of the new strontium uranyl selenites, $\text{Sr}[(\text{UO}_2)_3(\text{SeO}_3)_2\text{O}_2] \cdot 4\text{H}_2\text{O}$ and $\text{Sr}[(\text{UO}_2)(\text{SeO}_3)_2]$. *Am. Mineral.* **2004**, *89*, 976–980. [[CrossRef](#)]
39. Serezhkina, L.B.; Vologzhanina, A.V.; Marukhnov, A.V.; Pushkin, D.V.; Serezhkin, V.N. Synthesis and crystal structure of $\text{Na}_3(\text{H}_3\text{O})[(\text{UO}_2)(\text{SeO}_3)_2]_2 \cdot \text{H}_2\text{O}$. *Crystallogr. Rep.* **2009**, *54*, 852–857. [[CrossRef](#)]
40. Koskenlinna, M.; Valkonen, J. Ammonium uranyl hydrogenselenite selenite. *Acta Crystallogr.* **1996**, *52*, 1857–1859. [[CrossRef](#)]
41. Almond, P.; Albrecht-Schmitt, T.E. Hydrothermal syntheses, structures, and properties of the new uranyl selenites $\text{Ag}_2(\text{UO}_2)(\text{SeO}_3)_2$, $\text{M}[(\text{UO}_2)(\text{HSeO}_3)(\text{SeO}_3)]$ ($\text{M} = \text{K}, \text{Rb}, \text{Cs}, \text{Tl}$), and $\text{Pb}(\text{UO}_2)(\text{SeO}_3)_2$. *Inorg. Chem.* **2002**, *41*, 1177–1183. [[CrossRef](#)]
42. Meredith, N.A.; Polinski, M.J.; Lin, J.; Simonetti, A.; Albrecht-Schmitt, T.E. Incorporation of Neptunium(VI) into a uranyl selenite. *Inorg. Chem.* **2012**, *51*, 10480–10482. [[CrossRef](#)]
43. Burns, W.L.; Ibers, J.A. Syntheses and structures of three f-element selenite/hydroselenite compounds. *J. Solid State Chem.* **2009**, *182*, 1457–1461. [[CrossRef](#)]
44. Marukhnov, A.V.; Pushkin, D.V.; Peresypkina, E.V.; Virovets, A.V.; Serezhkina, L.B. Synthesis and structure of $\text{Na}[(\text{UO}_2)(\text{SeO}_3)(\text{HSeO}_3)](\text{H}_2\text{O})_4$. *Rus. J. Inorg. Chem.* **2008**, *53*, 831–836. [[CrossRef](#)]
45. Krivovichev, S.V. Crystal chemistry of selenates with mineral-like structures: VII. The structure of $(\text{H}_3\text{O})[(\text{UO}_2)(\text{SeO}_4)(\text{SeO}_2\text{OH})]$ and some structural features of selenite-selenates. *Geol. Ore Depos.* **2009**, *51*, 663–667. [[CrossRef](#)]
46. Wylie, E.M.; Burns, P.C. Crystal structures of six new uranyl selenate and selenite compounds and their relationship with uranyl mineral structures. *Can. Mineral.* **2012**, *50*, 147–157. [[CrossRef](#)]
47. Trombe, J.C.; Gleizes, A.; Galy, J. Structure of a uranyl diselenite, $\text{UO}_2\text{Se}_2\text{O}_5$. *Acta Crystallogr.* **1985**, *C41*, 1571–1573. [[CrossRef](#)]

48. Liu, D.-S.; Huang, G.-S.; Luo, Q.-Y.; Xu, Y.-P.; Li, X.-F. Poly[tetramethylammonium [nitratouranyl- μ_3 -selenito]]. *Acta Crystallogr.* **2006**, *E62*, 1584–1585.
49. Almond, P.M.; Albrecht-Schmitt, T.E. Do secondary and tertiary ammonium cations act as structure-directing agents in the formation of layered uranyl selenites? *Inorg. Chem.* **2003**, *42*, 5693–5698. [[CrossRef](#)]
50. Liu, D.S.; Kuang, H.M.; Chen, W.T.; Luo, Q.Y.; Sui, Y. Synthesis, structure, and photoluminescence properties of an organically-templated uranyl selenite. *Z. Anorg. Allg. Chem.* **2015**, *641*, 2009–2013. [[CrossRef](#)]
51. Krivovichev, S.V.; Tananaev, I.G.; Kahlenberg, V.; Myasoedov, B.F. Synthesis and crystal structure of the first uranyl Selenite(IV)-Selenate(VI) $[C_5H_{14}N][(UO_2)(SeO_4)(SeO_2OH)]$. *Dokl. Phys. Chem.* **2005**, *403*, 124–127. [[CrossRef](#)]
52. Gurzhiy, V.V.; Krivovichev, S.V.; Tananaev, I.G. Dehydration-driven evolution of topological complexity in ethylammonium uranyl selenates. *J. Solid State Chem.* **2017**, *247*, 105–112. [[CrossRef](#)]
53. Jouffret, L.J.; Wylie, E.M.; Burns, P.C. Influence of the organic species and Oxoanion in the synthesis of two uranyl sulfate hydrates, $(H_3O)_2[(UO_2)_2(SO_4)_3(H_2O)] \cdot 7H_2O$ and $(H_3O)_2[(UO_2)_2(SO_4)_3(H_2O)] \cdot 4H_2O$, and a uranyl Selenate-Selenite $[C_5H_6N][(UO_2)(SeO_4)(HSeO_3)]$. *Z. Anorg. Allg. Chem.* **2012**, *638*, 1796–1803. [[CrossRef](#)]
54. Gurzhiy, V.V.; Krivovichev, S.V.; Burns, P.C.; Tananaev, I.G.; Myasoedov, B.F. Supramolecular templates for the synthesis of new nanostructured uranyl compounds: Crystal structure of $[NH_3(CH_2)_9NH_3][(UO_2)(SeO_4)(SeO_2OH)](NO_3)$. *Radiochemistry* **2010**, *52*, 1–6. [[CrossRef](#)]
55. Kovrugin, V.M.; Gurzhiy, V.V.; Krivovichev, S.V.; Tananaev, I.G.; Myasoedov, B.F. Unprecedented layer topology in the crystal structure of a new organically templated uranyl selenite-selenate. *Mendeleev Commun.* **2012**, *22*, 11–12. [[CrossRef](#)]
56. Gurzhiy, V.V.; Kovrugin, V.M.; Tyumentseva, O.S.; Mikhailenko, P.A.; Krivovichev, S.V.; Tananaev, I.G. Topologically and geometrically flexible structural units in seven new organically templated uranyl selenates and selenite-selenates. *J. Solid State Chem.* **2015**, *229*, 32–40. [[CrossRef](#)]
57. Krivovichev, S.V.; Tananaev, I.G.; Kahlenberg, V.; Myasoedov, B.F. Synthesis and crystal structure of a new uranyl selenite(IV)-selenate(VI), $[C_5H_{14}N]_4[(UO_2)_3(SeO_4)_4(HSeO_3)(H_2O)](H_2SeO_3)(HSeO_4)$. *Radiochemistry* **2006**, *48*, 217–222. [[CrossRef](#)]
58. Wylie, E.M.; Smith, P.A.; Peruski, K.M.; Smith, J.S.; Dustin, M.K.; Burns, P.C. Effects of ionic liquid media on the cation selectivity of uranyl structural units in five new compounds produced using the ionothermal technique. *CrystEngComm* **2014**, *16*, 7236–7243. [[CrossRef](#)]
59. Gurzhiy, V.V.; Tyumentseva, O.S.; Tyshchenko, D.V.; Krivovichev, S.V.; Tananaev, I.G. Crown-ether-templated uranyl selenates: Novel family of mixed organic-inorganic actinide compounds. *Mendeleev Commun.* **2016**, *26*, 309–311. [[CrossRef](#)]
60. Gurzhiy, V.V.; Tyumentseva, O.S.; Britvin, S.N.; Krivovichev, S.V.; Tananaev, I.G. Ring opening of azetidine cycle: First examples of 1-azetidinepropanamine molecules as a template in hybrid organic-inorganic compounds. *J. Mol. Struct.* **2018**, *1151*, 88–96. [[CrossRef](#)]
61. Kovrugin, V.M.; Colmont, M.; Siidra, O.I.; Gurzhiy, V.V.; Krivovichev, S.V.; Mentre, O. Pathways for synthesis of new selenium-containing oxo-compounds: Chemical vapor transport reactions, hydrothermal techniques and evaporation method. *J. Cryst. Growth* **2017**, *457*, 307–313. [[CrossRef](#)]
62. Kovrugin, V.M.; Colmont, M.; Terry, C.; Colis, S.; Siidra, O.I.; Krivovichev, S.V.; Mentre, O. pH controlled pathway and systematic hydrothermal phase diagram for elaboration of synthetic lead nickel selenites. *Inorg. Chem.* **2015**, *54*, 2425–2434. [[CrossRef](#)]
63. Hawthorne, F.C.; Ferguson, R.B. Refinement of the crystal structure of kroehnkite. *Acta Crystallogr.* **1975**, *B31*, 1753–1755. [[CrossRef](#)]
64. Plášil, J.; Hlousek, J.; Kasatkin, A.V.; Novak, M.; Čejka, J.; Lapčák, L. Svornostite, $K_2Mg[(UO_2)(SO_4)_2] \cdot 8H_2O$, a new uranyl sulfate mineral from Jáchymov, Czech Republic. *J. Geosci.* **2015**, *60*, 113–121. [[CrossRef](#)]
65. Kampf, A.R.; Sejkora, J.; Witzke, T.; Plášil, J.; Čejka, J.; Nash, B.P.; Marty, J. Rietveldite, $Fe(UO_2)(SO_4)_2(H_2O)_5$, a new uranyl sulfate mineral from Giveaway-Simplot mine (Utah, USA), Willi Agatz mine (Saxony, Germany) and Jáchymov (Czech Republic). *J. Geosci.* **2017**, *62*, 107–120. [[CrossRef](#)]
66. Gurzhiy, V.V.; Tyumentseva, O.S.; Izatulina, A.R.; Krivovichev, S.V.; Tananaev, I.G. Chemically induced polytypic phase transitions in the $Mg[(UO_2)(TO_4)_2(H_2O)](H_2O)_4$ ($T = S, Se$) system. *Inorg. Chem.* **2019**, *58*, 14760–14768. [[CrossRef](#)] [[PubMed](#)]

67. Krivovichev, S.V.; Burns, P.C. First sodium uranyl chromate, $\text{Na}_4[(\text{UO}_2)(\text{CrO}_4)_3]$: Synthesis and crystal structure determination. *Z. Anorg. Allg. Chem.* **2003**, *629*, 1965–1968. [\[CrossRef\]](#)
68. Krivovichev, S.V.; Burns, P.C. Crystal chemistry of K uranyl chromates: Crystal structures of $\text{K}_8[(\text{UO}_2)(\text{CrO}_4)_4](\text{NO}_3)_2$, $\text{K}_5[(\text{UO}_2)(\text{CrO}_4)_3](\text{NO}_3)(\text{H}_2\text{O})_3$, $\text{K}_4[(\text{UO}_2)_3(\text{CrO}_4)_5](\text{H}_2\text{O})_8$ and $\text{K}_2[(\text{UO}_2)_2(\text{CrO}_4)_3(\text{H}_2\text{O})_2](\text{H}_2\text{O})_4$. *Z. Kristallogr.* **2003**, *218*, 725–732.
69. Krivovichev, S.V.; Burns, P.C. Crystal chemistry of uranyl molybdates. VIII. Crystal structures of $\text{Na}_3\text{Ti}_3[(\text{UO}_2)(\text{MoO}_4)_4]$, $\text{Na}_{13}\text{Ti}_3[(\text{UO}_2)(\text{MoO}_4)_3]_4(\text{H}_2\text{O})_5$, $\text{Na}_3\text{Ti}_5[(\text{UO}_2)(\text{MoO}_4)_3]_2(\text{H}_2\text{O})_3$ and $\text{Na}_2[(\text{UO}_2)(\text{MoO}_4)_2](\text{H}_2\text{O})_4$. *Can. Mineral.* **2003**, *41*, 707–720. [\[CrossRef\]](#)
70. Grigor'ev, M.S.; Fedoseev, A.M.; Budantseva, N.A.; Yanovskii, A.I.; Struchkov, Y.T.; Krot, N.N. Synthesis, crystal and molecular structure of complex neptunium(V) sulfates $(\text{Co}(\text{NH}_3)_6)(\text{NpO}_2(\text{SO}_4)_2) \cdot 2\text{H}_2\text{O}$ and $(\text{Co}(\text{NH}_3)_6) \text{H}_8\text{O}_3(\text{NpO}_2(\text{SO}_4)_3)$. *Sov. Radiokhem.* **1999**, *33*, 54–60.
71. Norquist, A.J.; Doran, M.B.; Thomas, P.M.; O'Hare, D. Structural diversity in organically templated sulfates. *Dalton Trans.* **2003**, 1168–1175. [\[CrossRef\]](#)
72. Forbes, T.Z.; Burns, P.C. Structures and syntheses of four Np^{5+} sulfate chain structures: Divergence from U^{6+} crystal chemistry. *J. Solid State Chem.* **2005**, *178*, 3455–3462. [\[CrossRef\]](#)
73. Gurchiy, V.V.; Tyumentseva, O.S.; Krivovichev, S.V.; Tananaev, I.G. Novel type of molecular connectivity in one-dimensional uranyl compounds: $[\text{K} @ (18\text{-crown-6})(\text{H}_2\text{O})][(\text{UO}_2)(\text{SeO}_4)(\text{NO}_3)]$, a new potassium uranyl selenate with 18-crown-6 ether. *Inorg. Chem. Commun.* **2014**, *45*, 93–96. [\[CrossRef\]](#)
74. Burns, P.C. A new uranyl phosphate chain in the structure of parsonsite. *Am. Mineral.* **2000**, *85*, 801–805. [\[CrossRef\]](#)
75. Locock, A.J.; Burns, P.C.; Flynn, T.M. The role of water in the structures of synthetic hallimondite, $\text{Pb}_2[(\text{UO}_2)(\text{AsO}_4)]_2(\text{H}_2\text{O})_n$ and synthetic parsonsite, $\text{Pb}_2[(\text{UO}_2)(\text{PO}_4)_2](\text{H}_2\text{O})_n$, $0 \leq n \leq 0.5$. *Am. Mineral.* **2005**, *90*, 240–246. [\[CrossRef\]](#)
76. Mills, S.J.; Birch, W.D.; Kolitsch, U.; Mumme, W.G.; Grey, I.E. Lakebogaite, $\text{CaNaFe}_2^{3+}\text{H}(\text{UO}_2)_2(\text{PO}_4)_4(\text{OH})_2(\text{H}_2\text{O})_8$, a new uranyl phosphate with a unique crystal structure from Victoria, Australia. *Am. Mineral.* **2008**, *93*, 691–697. [\[CrossRef\]](#)
77. Krivovichev, S.V.; Finch, R.; Burns, P.C. Crystal chemistry of uranyl molybdates. V. Topologically different uranyl molybdate sheets in structures of $\text{Na}_2[(\text{UO}_2)(\text{MoO}_4)_2]$ and $\text{K}_2[(\text{UO}_2)(\text{MoO}_4)_2](\text{H}_2\text{O})$. *Can. Mineral.* **2002**, *40*, 193–200. [\[CrossRef\]](#)
78. Grigor'ev, M.S.; Charushnikova, I.A.; Fedoseev, A.M.; Budantseva, N.A.; Yanovskii, A.I.; Struchkov, Y.T. Crystal and molecular structure of neptunium(V) complex molybdate $\text{K}_3\text{NpO}_2(\text{MoO}_4)_2$. *Sov. Radiokhem.* **1992**, *34*, 7–12.
79. Krivovichev, S.V.; Kahlenberg, V. Structural diversity of sheets in Rb uranyl selenates: Synthesis and crystal structures of $\text{Rb}_2[(\text{UO}_2)(\text{SeO}_4)_2(\text{H}_2\text{O})](\text{H}_2\text{O})$, $\text{Rb}_2[(\text{UO}_2)_2(\text{SeO}_4)_3(\text{H}_2\text{O})_2](\text{H}_2\text{O})_4$, $\text{Rb}_4[(\text{UO}_2)_3(\text{SeO}_4)_5(\text{H}_2\text{O})]$. *Z. Anorg. Allg. Chem.* **2005**, *631*, 739–744. [\[CrossRef\]](#)
80. Lussier, A.J.; Lopez, R.A.K.; Burns, P.C. A revised and expanded structure hierarchy of natural and synthetic hexavalent uranium compounds. *Can. Mineral.* **2016**, *54*, 177–283. [\[CrossRef\]](#)
81. Christ, C.L.; Clark, J.R.; Evans, H.T., Jr. Crystal structure of rutherfordine, UO_2CO_3 . *Science* **1955**, *121*, 472–473. [\[CrossRef\]](#)
82. Finch, R.J.; Cooper, M.A.; Hawthorne, F.C.; Ewing, R.C. Refinement of the crystal structure of rutherfordine. *Can. Mineral.* **1999**, *37*, 929–938.
83. Demartin, F.; Diella, V.; Donzelli, S.; Gramaccioli, C.M.; Pilati, T. The importance of accurate crystal structure determination of uranium minerals. I. Phosphuranylite $\text{KCa}(\text{H}_3\text{O})_3(\text{UO}_2)_7(\text{PO}_4)_4\text{O}_4 \cdot 8\text{H}_2\text{O}$. *Acta Crystallogr.* **1991**, *B47*, 439–446. [\[CrossRef\]](#)
84. Shvareva, T.Y.; Albrecht-Schmitt, T.E. General route to three-dimensional framework uranyl transition metal phosphates with atypical structural motifs: The case examples of $\text{Cs}_2\{[(\text{UO}_2)_4[\text{Co}(\text{H}_2\text{O})_2]_2(\text{HPO}_4)(\text{PO}_4)_4]\}$ and $\text{Cs}_{3+x}\{[(\text{UO}_2)_3\text{CuH}_{4-x}(\text{PO}_4)_5]\} \cdot \text{H}_2\text{O}$. *Inorg. Chem.* **2006**, *45*, 1900–1902. [\[CrossRef\]](#) [\[PubMed\]](#)
85. Plášil, J.; Hauser, J.; Petříček, V.; Meisser, N.; Mills, S.J.; Škoda, R.; Fejfarová, K.; Čejka, J.; Sejkora, J.; Hloušek, J.; et al. Crystal structure and formula revision of deliensite, $\text{Fe}[(\text{UO}_2)_2(\text{SO}_4)_2(\text{OH})_2](\text{H}_2\text{O})_7$. *Mineral. Mag.* **2012**, *76*, 2837–2860. [\[CrossRef\]](#)
86. Kampf, A.R.; Kasatkin, A.V.; Čejka, J.; Marty, J. Plášilite, $\text{Na}(\text{UO}_2)(\text{SO}_4)(\text{OH}) \cdot 2\text{H}_2\text{O}$, a new uranyl sulfate mineral from the Blue Lizard mine, San Juan County, Utah, USA. *J. Geosci.* **2015**, *60*, 1–10. [\[CrossRef\]](#)

87. Blatov, V.A.; Shevchenko, A.P.; Proserpio, D.M. Applied topological analysis of crystal structures with the program package ToposPro. *Cryst. Growth Des.* **2014**, *14*, 3576–3586. [\[CrossRef\]](#)
88. Guesdon, A.; Chardon, J.; Provost, J.; Raveau, B. A copper uranyl monophosphate built up from CuO_2 infinity chains: $\text{Cu}_2\text{UO}_2(\text{PO}_4)_2$. *J. Solid State Chem.* **2002**, *165*, 89–93. [\[CrossRef\]](#)
89. Krivovichev, S.V.; Burns, P.C. Synthesis and crystal structure of $\text{Li}_2[(\text{UO}_2)(\text{MoO}_4)_2]$, a uranyl molybdate with chains of corner-sharing uranyl square bipyramids and MoO_4 tetrahedra. *Solid State Sci.* **2003**, *5*, 481–485. [\[CrossRef\]](#)
90. Almond, P.M.; Albrecht-Schmitt, T.E. Expanding the remarkable structural diversity of uranyl tellurites: Hydrothermal preparation and structures of $\text{KUO}_2\text{Te}_2\text{O}_5(\text{OH})$, $\text{Ti}_3\{(\text{UO}_2)_2\text{Te}_2\text{O}_5(\text{OH})(\text{Te}_2\text{O}_6)\} \cdot 2\text{H}_2\text{O}$, $\beta\text{-Ti}_2(\text{UO}_2(\text{TeO}_3))_2$, and $\text{Sr}_3((\text{UO}_2)(\text{TeO}_3))_2(\text{TeO}_3)_2$. *Inorg. Chem.* **2002**, *41*, 5495–5501. [\[CrossRef\]](#)
91. Charykova, M.V.; Krivovichev, V.G. Mineral systems and the thermodynamics of selenites and selenates in the oxidation zone of sulfide ores—A review. *Mineral. Petrol.* **2017**, *111*, 121–134. [\[CrossRef\]](#)
92. Krivovichev, V.G.; Charykova, M.V.; Vishnevsky, A.V. The thermodynamics of selenium minerals in near-surface environments. *Minerals* **2017**, *7*, 188. [\[CrossRef\]](#)



© 2019 by the authors. Licensee MDPI, Basel, Switzerland. This article is an open access article distributed under the terms and conditions of the Creative Commons Attribution (CC BY) license (<http://creativecommons.org/licenses/by/4.0/>).